

TAMUNA: Doubly Accelerated Distributed Optimization with Local Training, Compression, and Partial Participation

Laurent Condat^{1,2} Ivan Agarský^{3,4} Grigory Malinovsky¹ Peter Richtárik^{1,2}

¹Computer Science Program, CEMSE Division,
King Abdullah University of Science and Technology (KAUST)
Thuwal, 23955-6900, Kingdom of Saudi Arabia

²SDAIA-KAUST Center of Excellence in Data Science
and Artificial Intelligence (SDAIA-KAUST AI)

³Brno University of Technology
Brno, Czech Republic

⁴Kempelen Institute of Intelligent Technologies (KInIT)
Bratislava, Slovakia

May 2023. Minor revision in April 2024

Abstract

In distributed optimization and learning, several machines alternate between local computations in parallel and communication with a distant server. Communication is usually slow and costly and forms the main bottleneck. This is particularly true in federated learning, where a large number of users collaborate toward a global training task. In addition, it is desirable for a robust algorithm to allow for partial participation, since it is often the case that some clients are not able to participate to the entire process and are idle at certain times. Two strategies are popular to reduce the communication burden: 1) local training, which consists in communicating less frequently, or equivalently performing more local computations between the communication rounds; and 2) compression, whereby compressed information instead of full-dimensional vectors is communicated. We propose TAMUNA, the first algorithm for distributed optimization that leveraged the two strategies of local training and compression jointly and allows for partial participation. In the strongly convex setting, TAMUNA converges linearly to the exact solution and provably benefits from the two mechanisms: it exhibits a doubly-accelerated convergence rate, with respect to the condition number of the functions and the model dimension.

Contents

1	Introduction	3
1.1	Formalism	3
1.2	A model of Asymmetric Communication	4
2	Related Work	5
2.1	Local Training (LT)	5
2.2	Partial Participation (PP)	6
2.3	Communication Compression (CC)	7
3	Challenges and Contributions	7
3.1	Combining LT and PP	7
3.2	Combining LT and CC	8
4	Proposed Algorithm TAMUNA	10
4.1	Iteration and Communication Complexities	13
5	Experiments	15
6	Conclusion	18
A	Proof of Theorem 1	23
A.1	The Random Variable \mathbf{d}^t	28
A.2	From Algorithm 2 to TAMUNA	30
B	Proof of Theorem 3	32
C	Sublinear Convergence in the Convex Case	33

1 Introduction

In traditional machine learning methods relying on a large amount of data, the data is first gathered and centralized in a datacenter before being processed. By contrast, in the recent paradigm of Federated Learning (FL) [Konečný et al., 2016a,b, McMahan et al., 2017, Bonawitz et al., 2017], a model is trained in a collaborative way, based on the wealth of information stored on edge devices, such as mobile phones, sensors and hospital workstations, without this private data being shared. This raises a multitude of challenges, to secure the process and maintain data privacy [Kairouz et al., 2021, Li et al., 2020a, Wang et al., 2021]. The devices perform computations locally in parallel and communicate back and forth with a distant orchestrating server, which aggregates the information and synchronizes the process so that a consensus is reached and a globally-optimal model is learnt. Communication between the parallel workers and the server, which takes place over the internet or cell phone network, is typically slow, costly, and unreliable. Thus, communication is the main bottleneck in this framework and forms the main challenge to be addressed by the community, before FL can be widely adopted.

Two strategies are popular to reduce the communication burden: 1) local training, which consists in communicating less frequently, or equivalently performing more local computations between the communication rounds; and 2) compression, whereby compressed information instead of full-dimensional vectors is communicated. Moreover, in practical applications where FL is deployed, it is unrealistic to assume that all clients are available 100% of the time to perform the required computation and communication operations. Thus, partial participation is an essential feature in practice, whereby only part of the clients need to participate in any given round of the process, while maintaining the overall convergence guarantees. We review existing methods using local training, compression, and allowing for partial participation in Section 2. In Section 3, we explain the challenges of combining these mechanisms and how we overcame them.

Our proposed randomized algorithm **TAMUNA** for communication-efficient distributed optimization and learning, presented in Section 4, combines local training and compression, and allows for partial participation. Being variance-reduced [Hanzely and Richtárik, 2019, Gorbunov et al., 2020a, Gower et al., 2020], it converges to an exact solution when exact gradients are called. The main feat is that **TAMUNA** provably benefits from the two mechanisms: the convergence rate is doubly accelerated, with respect to the condition number of the functions and the model dimension. In the remainder of this section, we formulate the setup and we propose a new model to characterize the communication complexity,

1.1 Formalism

We consider the classical client-server setup, with $n \geq 2$ clients doing computations in parallel and communicating back and forth with a server. We study the finite-sum optimization problem

$$\underset{x \in \mathbb{R}^d}{\text{minimize}} \quad f(x) := \frac{1}{n} \sum_{i=1}^n f_i(x), \tag{1}$$

where $f_i : \mathbb{R}^d \rightarrow \mathbb{R}$ is the individual loss function of client $i \in [n] := \{1, \dots, n\}$. This problem (1) is of utmost importance as it models empirical risk minimization, the dominant framework in supervised machine learning. In spite of its simple form, it is challenging because the number n of clients, as well as the dimension $d \geq 1$ of the model, can be very large.

Every function f_i is assumed to be \mathcal{L} -smooth and μ -strongly convex,¹ for some $\mathcal{L} \geq \mu > 0$. By strong convexity, the sought solution x^* of (1) exists and is unique. We define $\kappa := \frac{\mathcal{L}}{\mu}$. A sublinear convergence result is derived in the Appendix for the general convex case. We focus on the strongly convex case because the analysis of linear convergence rates provides clear insights on the mathematical and algorithmic mechanisms under study, namely local training, compression, and partial participation. We emphasize that the problem can be arbitrarily heterogeneous: we do not make any assumption on the functions f_i beyond smoothness and strong convexity, and there is no notion of data similarity whatsoever. We note that studying the minimization of a sum of nonconvex functions requires significantly different proof techniques [Karimireddy et al., 2021, Das et al., 2022], so the nonconvex setting is out of the scope of this paper. Moreover, whether variance-reduced algorithms are appropriate for deep learning, and nonconvex optimization in general, is still an open question in the community [Defazio and Bottou, 2019].

The basic algorithm of Gradient Descent (**GD**) solves the problem (1) by iterating, for $t = 0, 1, \dots$,

$$x^{t+1} := x^t - \frac{\gamma}{n} \sum_{i=1}^n \nabla f_i(x^t),$$

for some stepsize $\gamma \in (0, \frac{2}{\mathcal{L}})$. Iteration t proceeds as follows: first, x^t is broadcast by the server to all clients. Second, the clients compute the gradients $\nabla f_i(x^t)$ and send them to the server, in parallel. Third, the server averages the received vectors as $\nabla f(x^t) = \frac{1}{n} \sum_{i=1}^n \nabla f_i(x^t)$ and performs the gradient descent step $x^{t+1} = x^t - \gamma \nabla f(x^t)$. As is well known, for $\gamma = \Theta(\frac{1}{\mathcal{L}})$, **GD** converges linearly and reaches ϵ -accuracy with $\mathcal{O}(\kappa \log \epsilon^{-1})$ iterations. Since d -dimensional vectors are communicated at every iteration, the communication complexity of **GD** in number of reals is $\mathcal{O}(d\kappa \log \epsilon^{-1})$. Our goal is a twofold acceleration of **GD** with a better dependency to both κ and d in this complexity.

1.2 A model of Asymmetric Communication

We define **uplink communication (UpCom)** as the communication of information in parallel from the clients to the server, and **downlink communication (DownCom)** as the broadcast of the same message from the server to the clients:

$$\begin{aligned} &\text{uplink communication (UpCom) : clients to server} \\ &\text{downlink communication (DownCom) : server to clients} \end{aligned}$$

UpCom is typically much slower than DownCom, like uploading is slower than downloading on the internet or cell phone network. This can be due to the asymmetry of the service provider's systems or protocols used on the communication network, or constraints on the cache memory and aggregation speed of the server, which during UpCom has to decode and process the large number n of vectors received from the clients at the same.

We measure the uplink or downlink **communication complexity** as the expected number of communication rounds to reach ϵ -accuracy multiplied by the number of real numbers (floats) sent during a communication round between the server and any client. For instance, the UpCom or

¹A function $f : \mathbb{R}^d \rightarrow \mathbb{R}$ is said to be \mathcal{L} -smooth if it is differentiable and its gradient is Lipschitz continuous with constant \mathcal{L} ; that is, for every $x, y \in \mathbb{R}^d$, $\|\nabla f(x) - \nabla f(y)\| \leq \mathcal{L}\|x - y\|$ (we use the Euclidean norm throughout the paper). f is said to be μ -strongly convex if $f - \frac{\mu}{2}\|\cdot\|^2$ is convex. We refer to Bauschke and Combettes [2017] for such standard notions of convex analysis.

DownCom complexity of **GD** is $\mathcal{O}(d\kappa \log \epsilon^{-1})$. We could count bits, instead of floats, but since a float is typically represented in the IEEE floating-point standard using a fixed number, say 32, of bits, this is just a constant factor that does not change the asymptotic complexity.

Since UpCom is usually slower than DownCom, we propose to measure, like in Condat et al. [2022a], the **total communication (TotalCom)** complexity as a weighted sum of the UpCom and DownCom complexities:

$$\text{TotalCom} = \text{UpCom} + \alpha \cdot \text{DownCom}, \quad (2)$$

for some weight $\alpha \in [0, 1]$. A symmetric but unrealistic communication regime corresponds to $\alpha = 1$, whereas ignoring downCom and focusing on UpCom only, since UpCom is typically the limiting factor, corresponds to $\alpha = 0$. We will provide explicit expressions of the parameter values and TotalCom complexity for any given $\alpha \in [0, 1]$. So, our model is richer than only considering UpCom with $\alpha = 0$, as is the case in many papers on the topic of communication-efficient methods. Nevertheless, realistic values of α are small.

2 Related Work

In this section, we review the literature on the two main approaches used to decrease communication:

1) **Local Training (LT)**, which consists in communicating less frequently than after every GD step, or equivalently performing more local computations between successive communication rounds in order to send “richer” information to the server.

2) **Communication Compression (CC)**, which consists in sending shorter messages than full vectors made of d floats.

We also review existing work on **Partial Participation (PP)**.

2.1 Local Training (LT)

In GD, the gradient vectors are sent to the server right after being computed. LT is the simple but very effective idea of doing more computation than just one GD step before sending information to the server. Skipping communication was initially just a heuristic idea implemented in the **FedAvg** algorithm of McMahan et al. [2017] to reduce communication, but ample empirical evidence showed its practical efficiency, so that **FedAvg** became very popular. No theory was available to back up this technique, though. LT was first analyzed in the homogeneous, or i.i.d. data, regime, or under assumptions such as bounded gradient diversity [Haddadpour and Mahdavi, 2019]. It was then studied in the heterogeneous regime, which is more representative of FL [Khaled et al., 2019, Stich, 2019, Khaled et al., 2020, Li et al., 2020b, Woodworth et al., 2020, Gorbunov et al., 2021, Glasgow et al., 2022]. If too many GD steps are made, the local models get closer and closer to the minimizers of the local cost functions f_i , which are all different from each other and different from the global solution x^* . This so-called client drift was characterized in Malinovsky et al. [2020]. The LT methods of the next generation, including **Scaffold** [Karimireddy et al., 2020], **S-Local-GD** [Gorbunov et al., 2021] and **FedLin** [Mitra et al., 2021], were variance-reduced, with control variates used to correct for the client drift. They converge linearly to the exact solution, but their communication complexity is still $\mathcal{O}(d\kappa \log \epsilon^{-1})$, just like **GD**.

Most recently, a breakthrough was made with the appearance of *accelerated* LT methods. **Scaffnew**, proposed by Mishchenko et al. [2022], is the first LT-based algorithm achieving $\mathcal{O}(d\sqrt{\kappa} \log \epsilon^{-1})$ accelerated communication complexity. In **Scaffnew**, communication is triggered randomly with a

small probability p at every iteration. Thus, the expected number of local GD steps between two communication rounds is $1/p$. By choosing $p = 1/\sqrt{\kappa}$, the optimal dependency on $\sqrt{\kappa}$ instead of κ [Scaman et al., 2019] is obtained. **Scaffnew** has been extended in Malinovsky et al. [2022], using calls to variance-reduced [Gorbunov et al., 2020a, Gower et al., 2020] stochastic gradient estimates instead of exact gradients. It has also been analyzed in Condat and Richtárik [2023] as a particular case of **RandProx**, a primal-dual algorithm with a general randomized and variance-reduced dual update. Conceptually, our proposed algorithm **TAMUNA** is inspired by **RandProx**, with the dual update corresponding to the intermittent update of the control variates of the participating clients. **TAMUNA** is not a particular case of **RandProx**, though, because the primal update of the model and the dual update of the control variates are decoupled.

A different approach was developed by Sadiev et al. [2022a] with the **APDA-Inexact** algorithm, and then by Grudzień et al. [2023] with the **5GCS** algorithm: in both algorithms, the local steps correspond to an inner loop to compute a proximity operator inexactly.

TAMUNA relies on the same LT mechanism as **Scaffnew** and benefits from its accelerated dependency on $\sqrt{\kappa}$. However, we go even further and tackle the multiplicative factor d in the complexity, using compression.

2.2 Partial Participation (PP)

PP, a.k.a. client sampling, is the property that not all clients need to participate in a given round, consisting of a series of local steps followed by communication with the server. This is an important feature for a FL method, since in practice, there are many reasons for which a client might be idle and unable to do any computation and communication for a certain period of time. PP in SGD-type methods is now well understood [Gower et al., 2019, Condat and Richtárik, 2022], but its combination with LT has remained unconvincing so far. **Scaffold** allows for LT and PP, but its communication complexity does not benefit from LT. The variance-reduced **FedVARP** algorithm with LT and PP has been proposed [Jhunjhunwala et al., 2022], for nonconvex problems and with a bounded global variance assumption that does not hold in our setting. **Scaffnew** does not allow for PP. This was the motivation for Grudzień et al. [2023] to develop **5GCS**, which is, to the best of our knowledge, the first and only algorithm enabling LT and PP, and enjoying accelerated communication. We refer to Grudzień et al. [2023] for a detailed discussion of the literature of LT and PP. **5GCS** is completely different from **Scaffnew** and based on **Point-SAGA** [Defazio, 2016] instead of **GD**. Thus, it is an indirect, or two-level, combination of LT and PP: PP comes from the random selection of the activated proximity operators, whereas LT corresponds to an inner loop to compute these proximity operators inexactly. **TAMUNA** is a direct combination of LT and PP as two intertwined stochastic processes, and the first generalization of **Scaffnew** to PP.

Throughout the paper, we denote by $c \in \{2, \dots, n\}$ the cohort size, or number of active clients participating in every round. We report in Table 1 the communication complexity of the two known algorithms converging linearly to the exact solution, while allowing for LT and PP, namely **Scaffold** and **5GCS**. **Scaffold** is not accelerated, with a complexity depending on κ , and **5GCS** is accelerated with respect to κ but not d . Also, in **5GCS** the number of local steps in each communication round is of order at least $(\sqrt{\frac{cK}{n}} + 1) \log \kappa$, whereas in **TAMUNA** it is typically much smaller, of order $\sqrt{\frac{sK}{n}} + 1$ where s can be as small as 2, see (14).

2.3 Communication Compression (CC)

Another widely-used strategy to decrease the communication load is to make use of (lossy) compression. It can be formulated as follows: a possibly randomized compression operator $\mathcal{C} : \mathbb{R}^d \rightarrow \mathbb{R}^d$ is applied to the vector x to communicate, with the property that $\mathcal{C}(x)$ has a much more compact representation than the full vector $x \in \mathbb{R}^d$. \mathcal{C} is unbiased if $\mathbb{E}[\mathcal{C}(x)] = x$ for every $x \in \mathbb{R}^d$, where $\mathbb{E}[\cdot]$ denotes the expectation. Otherwise, it is biased. A popular unbiased compressor is **rand- k** , for some $k \in [d] := \{1, \dots, d\}$, which multiplies k elements of x , chosen uniformly at random, by d/k , and sets the other ones to zero. Only these k selected elements are actually communicated, usually with a few number of additional bits to encode which coordinates have been selected. k can be as small as 1 and the compression factor is d/k , which can be huge. Another sparsifying compressor is **top- k** , which keeps the k elements with largest absolute values and sets the other ones to zero [Beznosikov et al., 2020]. **top- k** is deterministic and biased.

A major milestone was the introduction of the variance-reduced algorithm **DIANA** [Mishchenko et al., 2019], which converges linearly with a large class of unbiased compressors. For example, when the clients use independent **rand-1** compressors for UpCom, the UpCom complexity of **DIANA** is $\mathcal{O}((\kappa(1 + \frac{d}{n}) + d) \log \epsilon^{-1})$. If n is large, the leading factor is $\kappa + d$, which is much better than $d\kappa$ with **GD**. **DIANA** has been extended in several ways [Horváth et al., 2022, Gorbunov et al., 2020a, Li et al., 2020c], including as a generalized version **DIANA-PP** allowing for PP [Condat and Richtárik, 2022]. However, the focus in **DIANA** is on UpCom and the full model is broadcast at every iteration, so that its TotalCom complexity can be *worse* than the one of **GD**. Extensions of **DIANA** with bidirectional CC, i.e. compression in both UpCom and DownCom, have been proposed [Gorbunov et al., 2020b, Philippenko and Dieuleveut, 2020, Liu et al., 2020, Condat and Richtárik, 2022], but this does not improve its TotalCom complexity; see also Philippenko and Dieuleveut [2021] and references therein on bidirectional CC. For biased compressors like **top- k** , the theory is less mature. The variance-reduced algorithm **EF21** [Richtárik et al., 2021, Fatkhullin et al., 2021, Condat et al., 2022b] converges linearly, but its complexity factor remains $d\kappa$, so it does not show any acceleration. Existing results are summarized in Table 2. Thus, compression alone is insufficient to obtain a communication-efficient algorithm and our proposed algorithm **TAMUNA** outperforms algorithms based solely on compression, thanks to its combination of LT and CC. We note that if LT is disabled ($L^{(r)} \equiv 1$), **TAMUNA** is still new and does not revert to a known algorithm with CC.

3 Challenges and Contributions

Let us look at the double challenge of combining LT with PP and CC. Our notations are summarized in Table 3 for convenience.

3.1 Combining LT and PP

With the recent breakthrough of **Scaffnew** [Mishchenko et al., 2022], we now understand that LT is not only efficient in practice, but also grounded in theory, and yields communication acceleration if the number of local steps is chosen appropriately. However, **Scaffnew** does not allow for PP. It has been an open and challenging question to know whether its powerful randomized mechanism would be compatible with PP. In fact, according to Grudzień et al. [2023], the authors of **Scaffnew** “*have tried—very hard in their own words—but their efforts did not bear any fruit.*” Combining LT and PP is difficult, because we want PP not only during communication, whenever it occurs, but also

Table 1: UpCom complexity ($\alpha = 0$) of linearly converging algorithms with LT or CC and allowing for PP (with exact gradients). The $\tilde{\mathcal{O}}$ notation hides the $\log \epsilon^{-1}$ factor (and other log factors for **Scaffold**). $c \in \{2, \dots, n\}$ is the number of participating clients and the other notations are recalled in Table 3.

Algorithm	LT	CC	UpCom
DIANA-PP ^(a)	✗	✓	$\tilde{\mathcal{O}}\left(\left(1 + \frac{d}{c}\right)\kappa + d\frac{n}{c}\right)$
Scaffold	✓	✗	$\tilde{\mathcal{O}}\left(d\kappa + d\frac{n}{c}\right)$
5GCS	✓	✗	$\tilde{\mathcal{O}}\left(d\sqrt{\kappa}\sqrt{\frac{n}{c}} + d\frac{n}{c}\right)$
TAMUNA	✓	✓	$\tilde{\mathcal{O}}\left(\sqrt{d}\sqrt{\kappa}\sqrt{\frac{n}{c}} + d\sqrt{\kappa}\sqrt{\frac{n}{c}} + d\frac{n}{c}\right)$

(a) using independent **rand-1** compressors, for instance. Note that $\mathcal{O}\left(\sqrt{d}\sqrt{\kappa}\sqrt{\frac{n}{c}} + d\frac{n}{c}\right)$ is better than $\mathcal{O}\left(\kappa + d\frac{n}{c}\right)$ and $\mathcal{O}\left(d\sqrt{\kappa}\sqrt{\frac{n}{c}} + d\frac{n}{c}\right)$ is better than $\mathcal{O}\left(\frac{d}{c}\kappa + d\frac{n}{c}\right)$, so that **TAMUNA** has a better complexity than **DIANA-PP**.

with respect to all computations before. The simple idea of allowing at every round some clients to be active and to proceed normally, and other clients to be idle with unchanged local variables, does not work. **TAMUNA** combines LT and PP successfully, and a key property in our design is that only the clients which participated in a given round make use of the updated model broadcast by the server to update their control variates (step 14). From a mathematical point of view, our approach relies on combining the two stochastic processes of probabilistic communication and random client selection *in two different ways*, for updating after communication the model estimates x_i on one hand, and the control variates h_i on the other hand. Indeed, a crucial property is that the sum of the control variates over all clients always remains zero. Thus, the model update and the control variate update are decoupled in **TAMUNA**, which fully benefits from the acceleration of LT, whatever the participation level; that is, its communication complexity depends on $\sqrt{\kappa}$, not κ .

3.2 Combining LT and CC

In the strongly convex and heterogeneous case considered here, the methods **Qsparse-local-SGD** [Basu et al., 2020] and **FedPAQ** [Reisizadeh et al., 2020] do not converge linearly. The only linearly converging LT + CC algorithm we are aware of is **FedCOMGATE** [Haddadpour et al., 2021]. But its rate is $\mathcal{O}(d\kappa \log \epsilon^{-1})$, which does not show any acceleration. We note that random reshuffling, which can be seen as a kind of LT, has been combined with CC in Sadiev et al. [2022b], Malinovsky and Richtárik [2022].

Thus, it is very challenging to combine LT and CC, just as it is to combine LT and PP, because in addition to client drift due to heterogeneity, there is another source of drift to be controlled. Simply “plugging” compressors into **Scaffnew** does not work, because the compression errors will propagate along the iterations. In algorithms like **DIANA** and **EF21**, the differences between local gradients and dedicated control variates are compressed. These differences converge to zero and the compression variance vanishes accordingly. This is possible because all gradients are computed at the same model estimate known by the server. But in an algorithm where multiple local steps have been performed and the local model estimates have drifted apart, the gradients are unusable. Also, compressing the differences between the current local estimates and the last global estimate known by the server does not work, because the latter is too old and this would ruin the benefits

Table 2: TotalCom complexity of linearly converging algorithms using Local Training (LT), Communication Compression (CC), or both, in case of full participation and exact gradients. The $\tilde{\mathcal{O}}$ notation hides the $\log \epsilon^{-1}$ factor. The notations are recalled in Table 3.

Algorithm	LT	CC	TotalCom	TotalCom=UpCom when $\alpha = 0$
DIANA ^(a)	✗	✓	$\tilde{\mathcal{O}}\left((1 + \alpha d + \frac{d + \alpha d^2}{n})\kappa + d + \alpha d^2\right)$	$\tilde{\mathcal{O}}\left(\left(1 + \frac{d}{n}\right)\kappa + d\right)$
EF21 ^(b)	✗	✓	$\tilde{\mathcal{O}}(d\kappa)$	$\tilde{\mathcal{O}}(d\kappa)$
Scaffold	✓	✗	$\tilde{\mathcal{O}}(d\kappa)$	$\tilde{\mathcal{O}}(d\kappa)$
FedLin	✓	✗	$\tilde{\mathcal{O}}(d\kappa)$	$\tilde{\mathcal{O}}(d\kappa)$
S-Local-GD	✓	✗	$\tilde{\mathcal{O}}(d\kappa)$	$\tilde{\mathcal{O}}(d\kappa)$
Scaffnew	✓	✗	$\tilde{\mathcal{O}}(d\sqrt{\kappa})$	$\tilde{\mathcal{O}}(d\sqrt{\kappa})$
5GCS	✓	✗	$\tilde{\mathcal{O}}(d\sqrt{\kappa})$	$\tilde{\mathcal{O}}(d\sqrt{\kappa})$
FedCOMGATE	✓	✓	$\tilde{\mathcal{O}}(d\kappa)$	$\tilde{\mathcal{O}}(d\kappa)$
TAMUNA	✓	✓	$\tilde{\mathcal{O}}\left(\sqrt{d}\sqrt{\kappa} + d\frac{\sqrt{\kappa}}{\sqrt{n}} + d + \sqrt{\alpha}d\sqrt{\kappa}\right)$	$\tilde{\mathcal{O}}\left(\sqrt{d}\sqrt{\kappa} + d\frac{\sqrt{\kappa}}{\sqrt{n}} + d\right)$

(a) using independent **rand-1** compressors, for instance. Note that $\mathcal{O}(\sqrt{d}\sqrt{\kappa} + d)$ is better than $\mathcal{O}(\kappa + d)$ and $\mathcal{O}(d\frac{\sqrt{\kappa}}{\sqrt{n}} + d)$ is better than $\mathcal{O}(\frac{d}{n}\kappa + d)$, so that **TAMUNA** has a better complexity than **DIANA**.

(b) using **top-k** compressors with any k , for instance.

of LT. So, the local model estimates themselves must be compressed. In our previous work, we designed a compression mechanism that is compatible with LT and proposed **CompressedScaffnew**, which enables CC in **Scaffnew** [Condat et al., 2022a]. This compression mechanism is based on permutations, so that the compressed messages sent by the different clients complement each other, to keep a tight control of the variance after aggregation. Its key property is that if all local model estimates to compress are equal, there is no compression error.

However, like **Scaffnew**, **CompressedScaffnew** only works in case of full participation. The successful combination of LT and CC in **CompressedScaffnew** does not help in combining LT and PP: a non-participating client does not participate to communication whenever it occurs, but it also does not perform any computation before. Therefore, there is no way to enable PP in loopless algorithms like **Scaffnew** and **CompressedScaffnew**, where communication can be triggered at any time. Our new algorithm **TAMUNA** is the first to solve this problem. Whether a client participates or not is decided at the beginning of a round consisting of a sequence of local steps followed by communication. **TAMUNA** works with any level of PP, with as few as two clients participating in every round. It relies on the same correction mechanism of client drift as **Scaffnew**, and uses the same permutation-based compressors as **CompressedScaffnew**, explained in Figure 1. However, **TAMUNA** has a different two-loop structure, to account for idle clients not computing and communicating for several successive iterations. It is an open question whether any other type of compressors can be used in **CompressedScaffnew** and **TAMUNA**, to apply for instance some form of quantization on top of sparsification [Horváth et al., 2022, Albasyoni et al., 2020].

TAMUNA establishes the new state of the art of communication-efficient algorithms enabling for PP. For instance, with exact gradients, if α is small and n is large, its TotalCom complexity in case of full participation is

$$\mathcal{O}\left(\left(\sqrt{d}\sqrt{\kappa} + d\right) \log \epsilon^{-1}\right),$$

Algorithm 1 TAMUNA

- 1: **input:** stepsizes $\gamma > 0$, $\eta > 0$; number of participating clients $c \in \{2, \dots, n\}$; sparsity index for compression $s \in \{2, \dots, c\}$; initial model estimate $\bar{x}^{(0)} \in \mathbb{R}^d$ at the server and initial control variates $h_1^{(0)}, \dots, h_n^{(0)} \in \mathbb{R}^d$ at the clients, such that $\sum_{i=1}^n h_i^{(0)} = 0$.
 - 2: **for** $r = 0, 1, \dots$ (rounds) **do**
 - 3: choose a subset $\Omega^{(r)} \subset [n]$ of size c uniformly at random
 - 4: choose the number of local steps $L^{(r)} \geq 1$
 - 5: **for** clients $i \in \Omega^{(r)}$, in parallel, **do**
 - 6: $x_i^{(r,0)} := \bar{x}^{(r)}$ (initialization received from the server)
 - 7: **for** $\ell = 0, \dots, L^{(r)} - 1$ (local steps) **do**
 - 8: $x_i^{(r,\ell+1)} := x_i^{(r,\ell)} - \gamma g_i^{(r,\ell)} + \gamma h_i^{(r)}$, where $g_i^{(r,\ell)}$ is an unbiased stochastic estimate of $\nabla f_i(x_i^{(r,\ell)})$ of variance σ_i^2
 - 9: **end for**
 - 10: **end for**
 - 11: UpCom: the server and active clients agree on a random binary mask $\mathbf{q}^{(r)} = (q_i^{(r)})_{i \in \Omega^{(r)}} \in \mathbb{R}^{d \times c}$ generated as explained in Figure 1, and every client $i \in \Omega^{(r)}$ sends the compressed vector $\mathcal{C}_i^{(r)}(x_i^{(r,L^{(r)})})$ to the server, where $\mathcal{C}_i^{(r)}(v)$ denotes v multiplied elementwise by $q_i^{(r)}$.
 - 12: $\bar{x}^{(r+1)} := \frac{1}{s} \sum_{i \in \Omega^{(r)}} \mathcal{C}_i^{(r)}(x_i^{(r,L^{(r)})})$ (aggregation by the server)
 - 13: **for** clients $i \in \Omega^{(r)}$, in parallel, **do**
 - 14: $h_i^{(r+1)} := h_i^{(r)} + \frac{\eta}{\gamma} (\mathcal{C}_i^{(r)}(\bar{x}^{(r+1)}) - \mathcal{C}_i^{(r)}(x_i^{(r,L^{(r)})})$ ($\bar{x}^{(r+1)}$ is received from the server)
 - 15: **end for**
 - 16: **for** clients $i \notin \Omega^{(r)}$, in parallel, **do**
 - 17: $h_i^{(r+1)} := h_i^{(r)}$ (the client is idle)
 - 18: **end for**
 - 19: **end for**
-

which shows the twofold acceleration, with $\sqrt{\kappa}$ instead of κ thanks to LT and \sqrt{d} instead of d thanks to CC. Our general result is in Theorem 3.

4 Proposed Algorithm TAMUNA

The proposed algorithm **TAMUNA** is shown as Algorithm 1. Its main loop is over the rounds, indexed by r . A round consists of a sequence, written as an inner loop, of local steps indexed by ℓ and performed in parallel by the active clients, followed by compressed communication with the server and update of the local control variates h_i . The c active, or participating, clients are selected randomly at the beginning of the round. During UpCom, every client sends a compressed version of its local model x_i : it sends only a few of its elements, selected randomly according to the rule explained in Figure 1 and known by both the clients and the server (for decoding).

At the end of the round, the aggregated model estimate $\bar{x}^{(r+1)}$ formed by the server is sent only to the active clients, which use it to update their control variates h_i . This update consists in overwriting only the coordinates of h_i which have been involved in the communication process; that is, for which the mask $q_i^{(r)}$ has a one. Indeed, the received vector $\bar{x}^{(r+1)}$ does not contain relevant

Table 3: Summary of the main notations used in the paper.

LT	local training
CC	communication compression
PP	partial participation (a.k.a. client sampling)
\mathcal{L}	smoothness constant
μ	strong convexity constant
$\kappa = \mathcal{L}/\mu$	condition number of the functions
d	dimension of the model
n, i	number and index of clients
$[n] = \{1, \dots, n\}$	
α	weight on downlink communication (DownCom), see (2)
$\sigma_i^2, \sigma^2 := \sum_i \sigma_i^2$	variance of the stochastic gradients, see (3)
$c \in \{2, \dots, n\}$	number of active clients (a.k.a. cohort size). Full participation if $c = n$
$\Omega \subset [n]$	index set of active clients
$s \in \{2, \dots, c\}$	sparsity index for compression. No compression if $s = c$
$\mathbf{q} = (q_i)_{i=1}^c$	random binary mask for compression, as detailed in Figure 1
r	index of rounds
L, ℓ	number and index of local steps in a round
p	inverse of the expected number of local steps per round
t, T	indexes of iterations
γ, η, χ	stepsizes
x_i	local model estimate at client i
h_i	local control variate tracking ∇f_i
$\bar{x}^{(r)}$	model estimate at the server at round r
τ	convergence rate

information to update h_i at the other coordinates.

The update of the local model estimates x_i at the clients takes place at the beginning of the round, when the active clients download the current model estimate $\bar{x}^{(r)}$ to initialize their local steps. So, it seems that there are two DownCom steps from the server to the clients per round (steps 6 and 14), but the algorithm can be written with only one: $\bar{x}^{(r+1)}$ can be broadcast by the server at the end of round r not only to the active clients of round r , but also to the active clients of the next round $r+1$, at the same time. We keep the algorithm written in this way for simplicity.

Thus, the clients of index $i \notin \Omega^{(r)}$, which do not participate in round r , are completely idle: they do not compute and do not communicate at all. Their local control variates h_i remain unchanged, and they do not even need to store a local model estimate: they only need to receive the latest model estimate $x^{(r)}$ from the server when they participate in the process.

In **TAMUNA**, unbiased stochastic gradient estimates of bounded variance σ_i^2 can be used: for every $i \in [n]$,

$$\mathbb{E} \left[g_i^{(r,\ell)} \mid x_i^{(r,\ell)} \right] = \nabla f_i(x_i^{(r,\ell)}), \quad \mathbb{E} \left[\left\| g_i^{(r,\ell)} - \nabla f_i(x_i^{(r,\ell)}) \right\|^2 \mid x_i^{(r,\ell)} \right] \leq \sigma_i^2, \quad (3)$$

for some $\sigma_i \geq 0$. We have $g_i^{(r,\ell)} = \nabla f_i(x_i^{(r,\ell)})$ if $\sigma_i = 0$. We define the total variance $\sigma^2 := \sum_{i=1}^n \sigma_i^2$. Our main result, stating linear convergence of **TAMUNA** to the exact solution x^* of (1), or to a

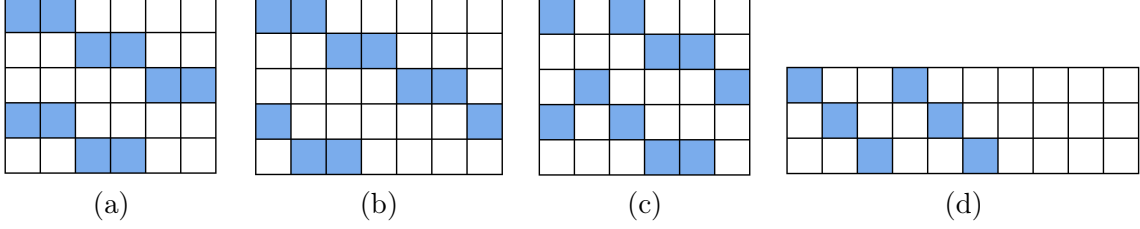


Figure 1: The random sampling pattern $\mathbf{q}^{(r)} = (q_i^{(r)})_{i=1}^c \in \mathbb{R}^{d \times c}$ used for communication is generated by a random permutation of the columns of a fixed binary template pattern, which has the prescribed number $s \geq 2$ of ones in every row. In (a) with $(d, c, s) = (5, 6, 2)$ and (b) with $(d, c, s) = (5, 7, 2)$, with ones in blue and zeros in white, examples of the template pattern used when $d \geq \frac{c}{s}$: for every row $k \in [d]$, there are s ones at columns $i = \text{mod}(s(k-1), c) + 1, \dots, \text{mod}(sk-1, c) + 1$. Thus, there are $\lfloor \frac{sd}{c} \rfloor$ or $\lceil \frac{sd}{c} \rceil$ ones in every column vector q_i . In (c), an example of sampling pattern obtained after a permutation of the columns of the template pattern in (a). In (d) with $(d, c, s) = (3, 10, 2)$, an example of the template pattern used when $\frac{c}{s} \geq d$: for every column $i = 1, \dots, ds$, there is 1 one at row $k = \text{mod}(i-1, d) + 1$. Thus, there is 0 or 1 one in every column vector q_i . We can note that when $d = \frac{c}{s}$, the two different rules for $d \geq \frac{c}{s}$ and $\frac{c}{s} \geq d$ for constructing the template pattern are equivalent, since they give exactly the same set of sampling patterns when permuting their columns. These two rules make it possible to generate easily the columns $q_i^{(r)}$ of $\mathbf{q}^{(r)}$ on the fly, without having to generate the whole mask $\mathbf{q}^{(r)}$ explicitly. This compression mechanism is the same as in **CompressedScaffnew** and this figure is the same as Figure 1 in our previous paper Condat et al. [2022a].

neighborhood if $\sigma > 0$, is the following:

Theorem 1 (fast linear convergence to a σ^2 -neighborhood). *Let $p \in (0, 1]$. In **TAMUNA**, suppose that at every round $r \geq 0$, $L^{(r)}$ is chosen randomly and independently according to a geometric law of mean p^{-1} ; that is, for every $L \geq 1$, $\text{Prob}(L^{(r)} = L) = (1-p)^{L-1}p$. Also, suppose that*

$$0 < \gamma < \frac{2}{\mathcal{L}} \quad (4)$$

and $\eta := p\chi$, where

$$0 < \chi \leq \frac{n(s-1)}{s(n-1)} \in \left(\frac{1}{2}, 1\right]. \quad (5)$$

For every total number $t \geq 0$ of local steps made so far, define the Lyapunov function

$$\bar{\Psi}^t := \frac{n}{\gamma} \|\bar{x}^t - x^*\|^2 + \frac{\gamma}{p^2\chi} \frac{n-1}{s-1} \sum_{i=1}^n \|h_i^{(r)} - h_i^*\|^2, \quad (6)$$

where x^* is the unique solution to (1), $h_i^* = \nabla f_i(x^*)$, $r \geq 0$ and $\ell \in \{0, \dots, L^{(r)} - 1\}$ are such that

$$t = \sum_{\hat{r}=0}^{r-1} L^{(\hat{r})} + \ell, \quad (7)$$

and

$$\bar{x}^t := \frac{1}{s} \sum_{i \in \Omega^{(r)}} C_i^{(r)}(x_i^{(r, \ell)}). \quad (8)$$

Then, for every $t \geq 0$,

$$\mathbb{E}[\bar{\Psi}^t] \leq \tau^t \bar{\Psi}^0 + \frac{\gamma \sigma^2}{1 - \tau}, \quad (9)$$

where

$$\tau := \max \left((1 - \gamma \mu)^2, (\gamma \mathcal{L} - 1)^2, 1 - p^2 \chi \frac{s-1}{n-1} \right) < 1. \quad (10)$$

Also, if $\sigma = 0$, $(\bar{x}^{(r)})_{r \in \mathbb{N}}$ converges to x^* and $(h_i^{(r)})_{r \in \mathbb{N}}$ converges to h_i^* , almost surely.

The complete proof is in the Appendix. We give a brief sketch here. We first analyze Algorithm 2, which has a single loop over the iterations indexed by t and one local step per iteration. Communication does not happen at every iteration but is only triggered randomly with probability p , like in **Scaffnew** and **CompressedScaffnew**. All clients perform computations at every iteration, and partial participation only concerns communication. In a second phase, we explain how Theorem 6 on Algorithm 2 yields the convergence proof of **TAMUNA** stated in Theorem 1. Since the contraction of the Lyapunov function happens at every iteration and not at every round, whose size is random, we have to reindex the local steps to obtain a rate depending on the number of iterations t so far.

We note that in (8), \bar{x}^t is actually computed only if $\ell = 0$, in which case $\bar{x}^t = \bar{x}^{(r)}$. We also note that the theorem depends on s but not on c . The dependence on c is hidden in the fact that s is upper bounded by c .

Remark 2 (setting η). *In the conditions of Theorem 1, one can simply set $\eta = \frac{p}{2}$ in **TAMUNA**, which is independent of n and s . However, the larger η , the better, so it is recommended to set*

$$\eta = p \frac{n(s-1)}{s(n-1)}. \quad (11)$$

Also, as a rule of thumb, if the average number of local steps per round is L , one can replace p by L^{-1} .

We can comment on the difference between **TAMUNA** and **Scaffold**, when CC is disabled ($s = c$). In **TAMUNA**, h_i is updated by adding $\bar{x}^{(r+1)} - x_i^{(r, L^{(r)})}$, the difference between the latest global estimate $\bar{x}^{(r+1)}$ and the latest local estimate $x_i^{(r, L^{(r)})}$. By contrast, in **Scaffold**, $\bar{x}^{(r)} - x_i^{(r, L^{(r)})}$ is used instead, which involves the “old” global estimate $\bar{x}^{(r)}$. Moreover, this difference is scaled by the number of local steps, which makes it small. That is why no acceleration from LT can be obtained in **Scaffold**, whatever the number of local steps. This is not a weakness of the analysis in Karimireddy et al. [2020] but an intrinsic limitation of **Scaffold**.

We can also note that the neighborhood size in (9) does not show so-called linear speedup; that is, it does not decrease when n increases. The properties of LT with SGD steps remain little understood [Woodworth et al., 2020], and we believe this should be studied within the general framework of variance reduction [Malinovsky et al., 2022]. This goes beyond the scope of this paper, which focuses on communication and not on the complexity of the local computations.

4.1 Iteration and Communication Complexities

We consider in this section that exact gradients are used ($\sigma = 0$),² since our aim is to establish a new state of the art for the communication complexity, regardless of the type of local computations.

²If $\sigma > 0$, it is possible to derive sublinear rates to reach ϵ -accuracy for the communication complexity, by setting γ proportional to ϵ , as was done for **Scaffnew** in Mishchenko et al. [2022, Corollary 5.6].

We place ourselves in the conditions of Theorem 1.

We first remark that **TAMUNA** has the same iteration complexity as **GD**, with rate $\tau^\# := \max(1 - \gamma\mu, \gamma\mathcal{L} - 1)^2$, as long as p and s are large enough to have $1 - \chi p^2 \frac{s-1}{n-1} \leq \tau^\#$. This is remarkable: LT, CC and PP do not harm convergence at all, until some threshold.

Let us consider the number of iterations (= total number of local steps) to reach ϵ -accuracy, i.e. $\mathbb{E}[\bar{\Psi}^t] \leq \epsilon$. For any $s \geq 2$, $p \in (0, 1]$, $\gamma = \Theta(\frac{1}{\mathcal{L}})$, and $\chi = \Theta(1)$, the iteration complexity of **TAMUNA** is

$$\mathcal{O}\left(\left(\kappa + \frac{n}{sp^2}\right) \log \epsilon^{-1}\right).$$

Thus, by choosing

$$p = \min\left(\Theta\left(\sqrt{\frac{n}{s\kappa}}\right), 1\right), \quad (12)$$

which means that the average number of local steps per round is

$$\mathbb{E}[L^{(r)}] = \max\left(\Theta\left(\sqrt{\frac{s\kappa}{n}}\right), 1\right), \quad (13)$$

the iteration complexity becomes

$$\mathcal{O}\left(\left(\kappa + \frac{n}{s}\right) \log \epsilon^{-1}\right).$$

We now consider the communication complexity. Communication occurs at every iteration with probability p , and during every communication round, DownCom consists in broadcasting the full d -dimensional vector $\bar{x}^{(r)}$, whereas in UpCom, compression is effective and the number of real values sent in parallel by the clients is equal to the number of ones per column in the sampling pattern \mathbf{q} , which is $\lceil \frac{sd}{c} \rceil \geq 1$. Hence, the communication complexities are:

$$\text{DownCom: } \mathcal{O}\left(pd\left(\kappa + \frac{n}{sp^2}\right) \log \epsilon^{-1}\right),$$

$$\text{UpCom: } \mathcal{O}\left(p\left(\frac{sd}{c} + 1\right)\left(\kappa + \frac{n}{sp^2}\right) \log \epsilon^{-1}\right).$$

$$\text{TotalCom: } \mathcal{O}\left(p\left(\frac{sd}{c} + 1 + \alpha d\right)\left(\kappa + \frac{n}{sp^2}\right) \log \epsilon^{-1}\right).$$

For a given s , the best choice for p , for both DownCom and UpCom, is given in (12), for which

$$\mathcal{O}\left(p\left(\kappa + \frac{n}{sp^2}\right)\right) = \mathcal{O}\left(\sqrt{\frac{n\kappa}{s}} + \frac{n}{s}\right)$$

and the TotalCom complexity is

$$\text{TotalCom: } \mathcal{O}\left(\left(\sqrt{\frac{n\kappa}{s}} + \frac{n}{s}\right)\left(\frac{sd}{c} + 1 + \alpha d\right) \log \epsilon^{-1}\right).$$

We see the first acceleration effect due to LT: with a suitable $p < 1$, the communication complexity only depends on $\sqrt{\kappa}$, not κ , whatever the participation level c and compression level s .

Without compression, i.e. $s = c$, whatever α , the TotalCom complexity becomes

$$\mathcal{O}\left(d\left(\sqrt{\frac{n\kappa}{c}} + \frac{n}{c}\right) \log \epsilon^{-1}\right).$$

We can now set s to further accelerate the algorithm, by minimizing the TotalCom complexity:

Theorem 3 (doubly accelerated communication). *In the conditions of Theorem 1, suppose that $\sigma = 0$, $\gamma = \Theta(\frac{1}{\epsilon})$, $\chi = \Theta(1)$, and*

$$p = \min\left(\Theta\left(\sqrt{\frac{n}{s\kappa}}\right), 1\right), \quad s = \max\left(2, \left\lfloor \frac{c}{d} \right\rfloor, \lfloor \alpha c \rfloor\right). \quad (14)$$

Then the TotalCom complexity of TAMUNA is

$$\mathcal{O}\left(\left(\sqrt{d}\sqrt{\kappa}\sqrt{\frac{n}{c}} + d\sqrt{\kappa}\frac{\sqrt{n}}{c} + d\frac{n}{c} + \sqrt{\alpha}d\sqrt{\kappa}\sqrt{\frac{n}{c}}\right) \log \epsilon^{-1}\right). \quad (15)$$

As reported in Tables 1 and 2, this complexity establishes the new state of the art.

Corollary 4 (dependence on α). *As long as $\alpha \leq \max(\frac{2}{c}, \frac{1}{d}, \frac{n}{\kappa c})$, there is no difference with the case $\alpha = 0$, in which we only focus on UpCom, and the TotalCom complexity is*

$$\mathcal{O}\left(\left(\sqrt{d}\sqrt{\kappa}\sqrt{\frac{n}{c}} + d\sqrt{\kappa}\frac{\sqrt{n}}{c} + d\frac{n}{c}\right) \log \epsilon^{-1}\right). \quad (16)$$

On the other hand, if $\alpha \geq \max(\frac{2}{c}, \frac{1}{d}, \frac{n}{\kappa c})$, the complexity increases and becomes

$$\mathcal{O}\left(\sqrt{\alpha}d\sqrt{\kappa}\sqrt{\frac{n}{c}} \log \epsilon^{-1}\right), \quad (17)$$

but compression remains operational and effective with the $\sqrt{\alpha}$ factor. It is only when $\alpha = 1$ that $s = c$, i.e. there is no compression, and that the Upcom, DownCom and TotalCom complexities all become

$$\mathcal{O}\left(d\sqrt{\kappa}\sqrt{\frac{n}{c}} \log \epsilon^{-1}\right). \quad (18)$$

Thus, in case of full participation ($c = n$), TAMUNA is faster than Scaffnew for every $\alpha \in [0, 1]$.

Corollary 5 (full participation). *In case of full participation ($c = n$), the TotalCom complexity of TAMUNA is*

$$\mathcal{O}\left(\left(\sqrt{d}\sqrt{\kappa} + d\frac{\sqrt{\kappa}}{\sqrt{n}} + d + \sqrt{\alpha}d\sqrt{\kappa}\right) \log \epsilon^{-1}\right). \quad (19)$$

5 Experiments

We illustrate our theoretical findings by experiments on a practical logistic regression problem. The global loss function is defined as

$$f(x) = \frac{1}{M} \sum_{m=1}^M \left(\log\left(1 + \exp\left(-b_m a_m^\top x\right)\right) + \frac{\mu}{2} \|x\|^2 \right), \quad (20)$$

where the variables $a_m \in \mathbb{R}^d$ and $b_m \in \{-1, 1\}$ represent the data samples, and M denotes the total number of samples. The function f in (20) is divided into n separate functions f_i , with any remainder from dividing M by n discarded. We select the strong convexity constant μ so that $\kappa = 10^4$.

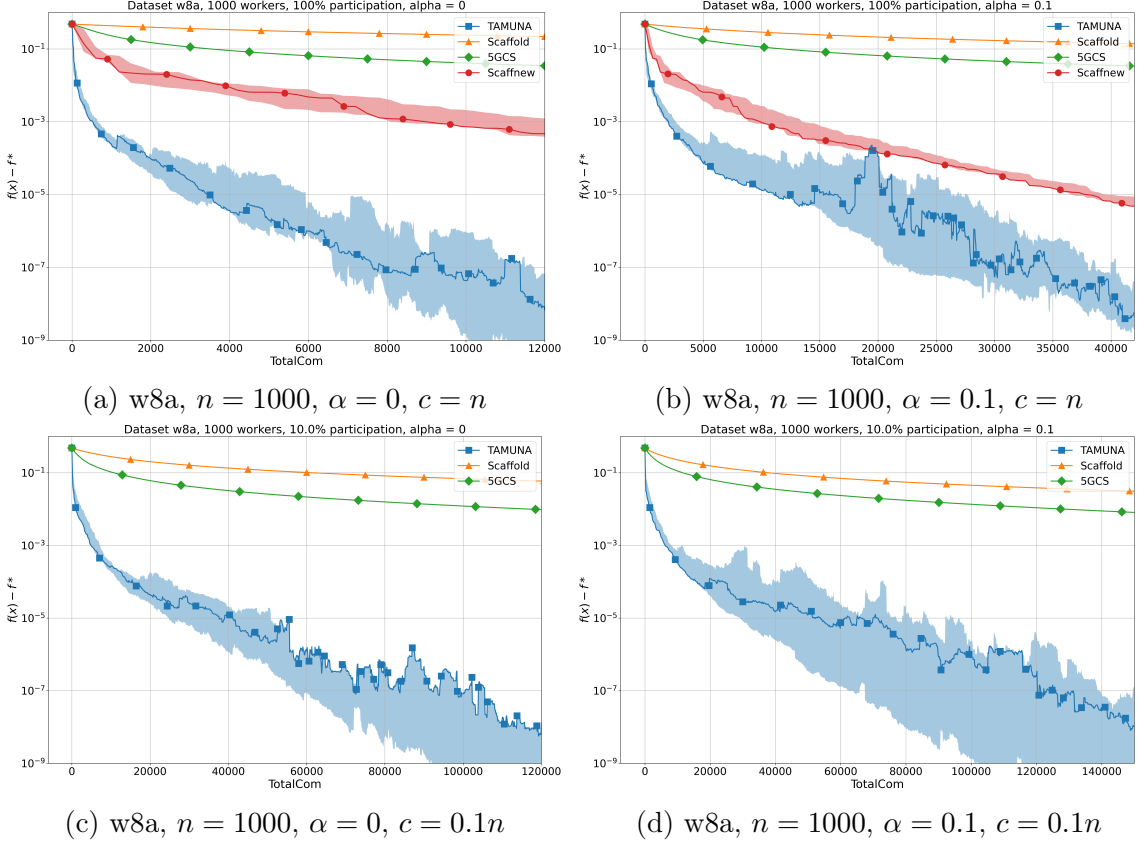


Figure 2: Logistic regression experiment in the case $n > d$. The dataset w8a has $d = 300$ features and $n = 1000$, so $n \approx 3d$. The first row shows a comparison in the full participation regime, while the second row shows a comparison in the partial participation regime with 10% of clients. On the left, $\alpha = 0$, while on the right, $\alpha = 0.1$.

For our analysis, we choose $n = 1000$ and examine two scenarios: in the first one, we have $d > n$ using the ‘real-sim’ dataset with $d = 20958$, and in the second one, we have $n > d$ using the ‘w8a’ dataset with $d = 300$, from the widely-used LIBSVM library [Chang and Lin, 2011]. Additionally, we consider two cases for each scenario: $\alpha = 0$ and $\alpha = 0.1$, where α is the weight on DownCom defined in (2).

We measure the convergence error $f(x) - f(x^*)$ with respect to TotalCom, i.e. the total number of communicated reals, as defined in Section (1.2). Here, x denotes the model known by the server; for TAMUNA, this is $\bar{x}^{(r)}$. This error serves as a natural basis for comparing algorithms, and since f is \mathcal{L} -smooth, we have $f(x) - f(x^*) \leq \frac{\mathcal{L}}{2} \|x - x^*\|^2$ for any x . Consequently, the error converges linearly at the same rate as Ψ in Theorem 1.

We compare the performance of three algorithms allowing for PP, namely Scaffold, 5GCS, and TAMUNA, for two participation scenarios: $c = n$ and $c = 0.1n$ (10% participation). In the full participation case, we add Scaffoldnew to the comparison.

In order to ensure theoretical conditions that guarantee linear convergence, we set γ and η for

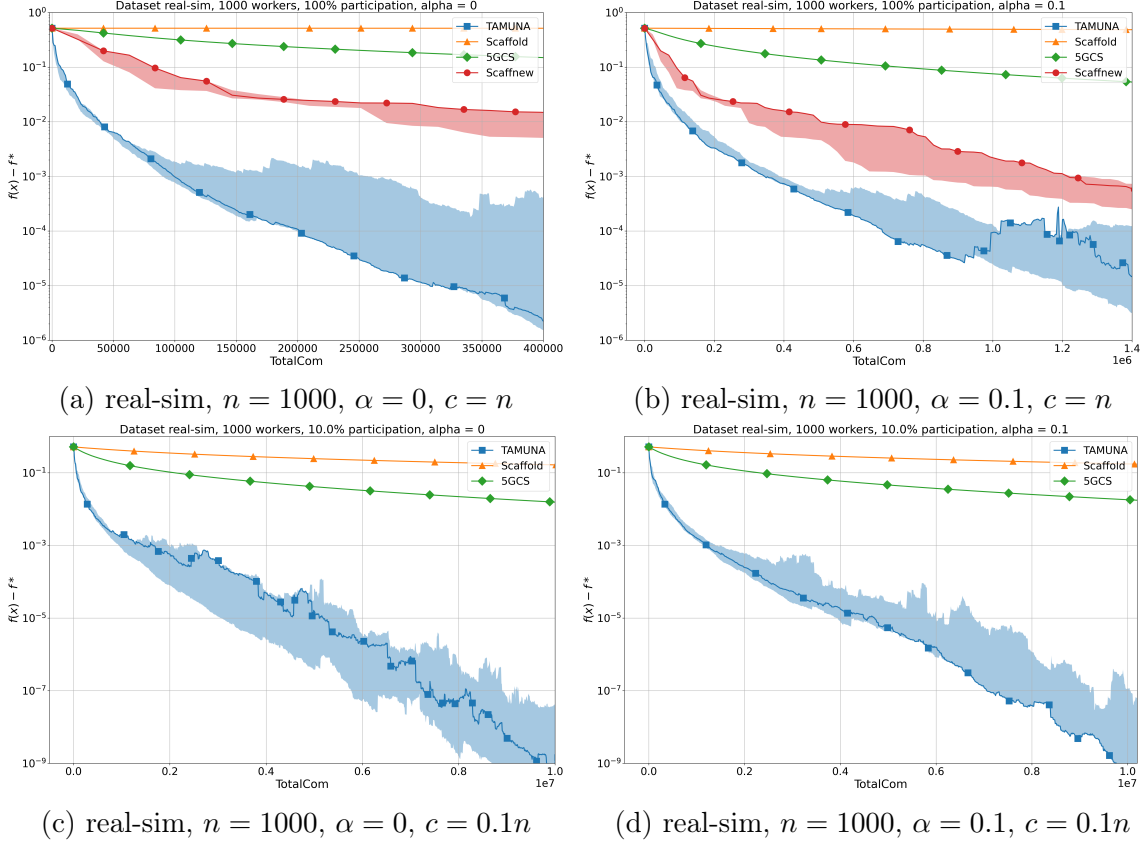


Figure 3: Logistic regression experiment in the case $d > n$. The dataset real-sim has $d = 20,958$ features and $n = 1000$, so $n \approx d/20$. The first row shows a comparison in the full participation regime, while the second row shows a comparison in the partial participation regime with 10% of clients. On the left, $\alpha = 0$, while on the right, $\alpha = 0.1$.

TAMUNA as

$$\gamma = \frac{2}{\mathcal{L} + \mu}, \quad \eta = p \frac{n(s-1)}{s(n-1)},$$

where the remaining parameters s and p are fine-tuned to achieve the best communication complexity. In our experimental setup, we found that using $s = 40$ and $p = 0.01$ resulted in excellent performance. The conditions of Theorem 1 are met with these values, so linear convergence of TAMUNA is guaranteed. We adopt the same values of γ and p for Scaffnew. For Scaffold, we use p^{-1} local steps, which is the same, on average, as for TAMUNA and Scaffnew; the behavior of Scaffold changed marginally with other values. We also set γ to its highest value that ensures convergence. In the case of 5GCS, we tune γ , τ , and the number of local steps to achieve the best communication complexity.

The models in all algorithms, as well as the control variates in TAMUNA, Scaffnew and Scaffold, are initialized with zero vectors.

The results are shown in Figures 2 and 3. Each algorithm is run multiple times with different random seeds, depending on its variance (7 times for TAMUNA, 5 times for Scaffnew, and 3 times for Scaffold and 5GCS). The shaded area in the plots shows the difference between the maximum

and minimum convergence error achieved over these runs. Additionally, the progress of the first run for each algorithm is depicted with a thicker line and markers.

As can be seen, our proposed algorithm **TAMUNA** outperforms all other methods. In case of full participation, **Scaffnew** outperforms **Scaffold** and **5GCS**, which shows the efficiency of its LT mechanism. **TAMUNA** embeds the same mechanism and also benefits from it, but it outperforms **Scaffnew** thanks to CC, its second communication-acceleration mechanism. The difference between **TAMUNA** and **Scaffnew** is larger for $\alpha = 0$ than for $\alpha = 0.1$, as explained by our theory; the difference would vanish if α tends to 1. **TAMUNA** is applicable and proved to converge with any level of PP, whereas **Scaffnew** only applies to the full participation case.

6 Conclusion

We introduced **TAMUNA**, the first communication-efficient algorithm that allows for partial participation (PP) and provably benefits from the two combined acceleration mechanisms of Local Training (LT) and Communication Compression (CC), in the convex setting. Moreover, this is achieved not only for uplink communication, but for our more comprehensive model of total communication. These theoretical guarantees are confirmed in practice and **TAMUNA** communicates less than existing algorithms to reach the same accuracy. An important venue for future work will be to generalize our specific compression mechanism to a broad class of compressors including quantization [Horváth et al., 2022]. Another venue consists in implementing internal variance reduction for the stochastic gradients, as was done for **Scaffnew** in Malinovsky et al. [2022].

Acknowledgement

This work was supported by the SDAIA-KAUST Center of Excellence in Data Science and Artificial Intelligence (SDAIA-KAUST AI).

References

- A. Albasyoni, M. Safaryan, L. Condat, and P. Richtárik. Optimal gradient compression for distributed and federated learning. preprint arXiv:2010.03246, 2020.
- D. Basu, D. Data, C. Karakus, and S. N. Diggavi. Qsparse-Local-SGD: Distributed SGD With Quantization, Sparsification, and Local Computations. *IEEE Journal on Selected Areas in Information Theory*, 1(1):217–226, 2020.
- H. H. Bauschke and P. L. Combettes. *Convex Analysis and Monotone Operator Theory in Hilbert Spaces*. Springer, New York, 2nd edition, 2017.
- D. P. Bertsekas. *Convex optimization algorithms*. Athena Scientific, Belmont, MA, USA, 2015.
- A. Beznosikov, S. Horváth, P. Richtárik, and M. Safaryan. On biased compression for distributed learning. preprint arXiv:2002.12410, 2020.
- K. Bonawitz, V. Ivanov, B. Kreuter, A. Marcedone, H. B. McMahan, S. Patel, D. Ramage, A. Segal, and K. Seth. Practical secure aggregation for privacy-preserving machine learning. In *Proc. of the*

- 2017 ACM SIGSAC Conference on Computer and Communications Security*, pages 1175–1191, 2017.
- C.-C. Chang and C.-J. Lin. LIBSVM: A library for support vector machines. *ACM Transactions on Intelligent Systems and Technology*, 2:27:1–27:27, 2011. Software available at <http://www.csie.ntu.edu.tw/%7Ecjlin/libsvm>.
- L. Condat and P. Richtárik. MURANA: A generic framework for stochastic variance-reduced optimization. In *Proc. of the conference Mathematical and Scientific Machine Learning (MSML)*, PMLR 190, pages 81–96, 2022.
- L. Condat and P. Richtárik. RandProx: Primal-dual optimization algorithms with randomized proximal updates. In *Proc. of Int. Conf. Learning Representations (ICLR)*, 2023.
- L. Condat, I. Agarský, and P. Richtárik. Provably doubly accelerated federated learning: The first theoretically successful combination of local training and compressed communication. preprint arXiv:2210.13277, 2022a.
- L. Condat, K. Li, and P. Richtárik. EF-BV: A unified theory of error feedback and variance reduction mechanisms for biased and unbiased compression in distributed optimization. In *Proc. of Conf. Neural Information Processing Systems (NeurIPS)*, 2022b.
- R. Das, A. Acharya, A. Hashemi, S. Sanghavi, I. S. Dhillon, and U. Topcu. Faster non-convex federated learning via global and local momentum. In *Proc. of Conf. on Uncertainty in Artificial Intelligence (UAI)*, 2022.
- A. Defazio. A simple practical accelerated method for finite sums. In *Proc. of 30th Conf. Neural Information Processing Systems (NIPS)*, volume 29, pages 676–684, 2016.
- A. Defazio and L. Bottou. On the ineffectiveness of variance reduced optimization for deep learning. In *Proc. of Conf. Neural Information Processing Systems (NeurIPS)*, 2019.
- I. Fatkhullin, I. Sokolov, E. Gorbunov, Z. Li, and P. Richtárik. EF21 with bells & whistles: Practical algorithmic extensions of modern error feedback. preprint arXiv:2110.03294, 2021.
- M. R. Glasgow, H. Yuan, and T. Ma. Sharp bounds for federated averaging (Local SGD) and continuous perspective. In *Proc. of Int. Conf. Artificial Intelligence and Statistics (AISTATS)*, PMLR 151, pages 9050–9090, 2022.
- E. Gorbunov, F. Hanzely, and P. Richtárik. A unified theory of SGD: Variance reduction, sampling, quantization and coordinate descent. In *Proc. of 23rd Int. Conf. Artificial Intelligence and Statistics (AISTATS)*, PMLR 108, 2020a.
- E. Gorbunov, D. Kovalev, D. Makarenko, and P. Richtárik. Linearly converging error compensated SGD. In *Proc. of Conf. Neural Information Processing Systems (NeurIPS)*, 2020b.
- E. Gorbunov, F. Hanzely, and P. Richtárik. Local SGD: Unified theory and new efficient methods. In *Proc. of 24th Int. Conf. Artificial Intelligence and Statistics (AISTATS)*, PMLR 130, pages 3556–3564, 2021.

- R. M. Gower, N. Loizou, X. Qian, A. Sailanbayev, E. Shulgin, and P. Richtárik. SGD: General analysis and improved rates. In *Proc. of 36th Int. Conf. Machine Learning (ICML)*, volume PMLR 97, pages 5200–5209, 2019.
- R. M. Gower, M. Schmidt, F. Bach, and P. Richtárik. Variance-reduced methods for machine learning. *Proc. of the IEEE*, 108(11):1968–1983, November 2020.
- M. Grudzień, G. Malinovsky, and P. Richtárik. Can 5th Generation Local Training Methods Support Client Sampling? Yes! In *Proc. of Int. Conf. Artificial Intelligence and Statistics (AISTATS)*, April 2023.
- F. Haddadpour and M. Mahdavi. On the Convergence of Local Descent Methods in Federated Learning. preprint arXiv:1910.14425, 2019.
- F. Haddadpour, M. M. Kamani, A. Mokhtari, and M. Mahdavi. Federated learning with compression: Unified analysis and sharp guarantees. In *Proc. of Int. Conf. Artificial Intelligence and Statistics (AISTATS)*, PMLR 130, pages 2350–2358, 2021.
- F. Hanzely and P. Richtárik. One method to rule them all: Variance reduction for data, parameters and many new methods. preprint arXiv:1905.11266, 2019.
- S. Horváth, C.-Y. Ho, L. Horváth, A. N. Sahu, M. Canini, and P. Richtárik. Natural compression for distributed deep learning. In *Proc. of the conference Mathematical and Scientific Machine Learning (MSML)*, PMLR 190, 2022.
- S. Horváth, D. Kovalev, K. Mishchenko, S. Stich, and P. Richtárik. Stochastic distributed learning with gradient quantization and variance reduction. *Optimization Methods and Software*, 2022.
- D. Jhunjunwala, P. Sharma, A. Nagarkatti, and G. Joshi. FedVARP: Tackling the variance due to partial client participation in federated learning. In *Proc. of 38th Conf. Uncertainty in Artificial Intelligence (UAI)*, volume PMLR 180, pages 906–916, 2022.
- P. Kairouz et al. Advances and open problems in federated learning. *Foundations and Trends in Machine Learning*, 14(1–2), 2021.
- S. P. Karimireddy, S. Kale, M. Mohri, S. Reddi, S. U. Stich, and A. T. Suresh. SCAFFOLD: Stochastic controlled averaging for federated learning. In *Proc. of 37th Int. Conf. Machine Learning (ICML)*, pages 5132–5143, 2020.
- S. P. Karimireddy, M. Jaggi, S. Kale, M. Mohri, S. Reddi, S. U. Stich, and A. T. Suresh. Breaking the centralized barrier for cross-device federated learning. In *Proc. of Conf. Neural Information Processing Systems (NeurIPS)*, 2021.
- A. Khaled, K. Mishchenko, and P. Richtárik. Better communication complexity for local SGD. In *NeurIPS Workshop on Federated Learning for Data Privacy and Confidentiality*, 2019.
- A. Khaled, K. Mishchenko, and P. Richtárik. Tighter theory for local SGD on identical and heterogeneous data. In *Proc. of 23rd Int. Conf. Artificial Intelligence and Statistics (AISTATS)*, PMLR 108, 2020.

- J. Konečný, H. B. McMahan, D. Ramage, and P. Richtárik. Federated optimization: distributed machine learning for on-device intelligence. arXiv:1610.02527, 2016a.
- J. Konečný, H. B. McMahan, F. X. Yu, P. Richtárik, A. T. Suresh, and D. Bacon. Federated learning: Strategies for improving communication efficiency. In *NIPS Private Multi-Party Machine Learning Workshop*, 2016b. arXiv:1610.05492.
- T. Li, A. K. Sahu, A. Talwalkar, and V. Smith. Federated learning: Challenges, methods, and future directions. *IEEE Signal Processing Magazine*, 3(37):50–60, 2020a.
- X. Li, K. Huang, W. Yang, S. Wang, and Z. Zhang. On the convergence of FedAvg on non-iid data. In *Proc. of Int. Conf. Learning Representations (ICLR)*, 2020b.
- Z. Li, D. Kovalev, X. Qian, and P. Richtárik. Acceleration for compressed gradient descent in distributed and federated optimization. In *Proc. of 37th Int. Conf. Machine Learning (ICML)*, volume PMLR 119, 2020c.
- X. Liu, Y. Li, J. Tang, and M. Yan. A double residual compression algorithm for efficient distributed learning. In *Proc. of Int. Conf. Artificial Intelligence and Statistics (AISTATS)*, PMLR 108, pages 133–143, 2020.
- G. Malinovsky and P. Richtárik. Federated random reshuffling with compression and variance reduction. preprint arXiv:arXiv:2205.03914, 2022.
- G. Malinovsky, D. Kovalev, E. Gasanov, L. Condat, and P. Richtárik. From local SGD to local fixed point methods for federated learning. In *Proc. of 37th Int. Conf. Machine Learning (ICML)*, volume PMLR 119, pages 6692–6701, 2020.
- G. Malinovsky, K. Yi, and P. Richtárik. Variance reduced ProxSkip: Algorithm, theory and application to federated learning. In *Proc. of Conf. Neural Information Processing Systems (NeurIPS)*, 2022.
- H. B. McMahan, E. Moore, D. Ramage, S. Hampson, and B. Agüera y Arcas. Communication-efficient learning of deep networks from decentralized data. In *Proc. of Int. Conf. Artificial Intelligence and Statistics (AISTATS)*, PMLR 54, 2017.
- K. Mishchenko, E. Gorbunov, M. Takáč, and P. Richtárik. Distributed learning with compressed gradient differences. arXiv:1901.09269, 2019.
- K. Mishchenko, G. Malinovsky, S. Stich, and P. Richtárik. ProxSkip: Yes! Local Gradient Steps Provably Lead to Communication Acceleration! Finally! In *Proc. of the 39th International Conference on Machine Learning (ICML)*, July 2022.
- A. Mitra, R. Jaafar, G. Pappas, and H. Hassani. Linear convergence in federated learning: Tackling client heterogeneity and sparse gradients. In *Proc. of Conf. Neural Information Processing Systems (NeurIPS)*, 2021.
- C. Philippenko and A. Dieuleveut. Artemis: tight convergence guarantees for bidirectional compression in federated learning. preprint arXiv:2006.14591, 2020.

- C. Philippenko and A. Dieuleveut. Preserved central model for faster bidirectional compression in distributed settings. In *Proc. of Conf. Neural Information Processing Systems (NeurIPS)*, 2021.
- A. Reisizadeh, A. Mokhtari, H. Hassani, A. Jadbabaie, and R. Pedarsani. FedPAQ: A communication-efficient federated learning method with periodic averaging and quantization. In *Proc. of Int. Conf. Artificial Intelligence and Statistics (AISTATS)*, pages 2021–2031, 2020.
- P. Richtárik, I. Sokolov, and I. Fatkhullin. EF21: A new, simpler, theoretically better, and practically faster error feedback. In *Proc. of 35th Conf. Neural Information Processing Systems (NeurIPS)*, 2021.
- A. Sadiev, D. Kovalev, and P. Richtárik. Communication acceleration of local gradient methods via an accelerated primal-dual algorithm with an inexact prox. In *Proc. of Conf. Neural Information Processing Systems (NeurIPS)*, 2022a.
- A. Sadiev, G. Malinovsky, E. Gorbunov, I. Sokolov, A. Khaled, K. Burlachenko, and P. Richtárik. Federated optimization algorithms with random reshuffling and gradient compression. preprint arXiv:2206.07021, 2022b.
- K. Scaman, F. Bach, S. Bubeck, Y. T. Lee, and L. Massoulié. Optimal convergence rates for convex distributed optimization in networks. *Journal of Machine Learning Research*, 20:1–31, 2019.
- S. U. Stich. Local SGD converges fast and communicates little. In *Proc. of International Conference on Learning Representations (ICLR)*, 2019.
- J. Wang et al. A field guide to federated optimization. preprint arXiv:2107.06917, 2021.
- B. E. Woodworth, K. K. Patel, and N. Srebro. Minibatch vs Local SGD for heterogeneous distributed learning. In *Proc. of Conf. Neural Information Processing Systems (NeurIPS)*, 2020.

Algorithm 2

1: **input:** stepsizes $\gamma > 0$, $\chi > 0$; probability $p \in (0, 1]$; number of participating clients $c \in \{2, \dots, n\}$; compression index $s \in \{2, \dots, c\}$; initial estimates $x_1^0, \dots, x_n^0 \in \mathbb{R}^d$ and $h_1^0, \dots, h_n^0 \in \mathbb{R}^d$ such that $\sum_{i=1}^n h_i^0 = 0$, sequence of independent coin flips $\theta^0, \theta^1, \dots$ with $\text{Prob}(\theta^t = 1) = p$, and for every t with $\theta^t = 1$, a subset $\Omega^t \subset [n]$ of size c chosen uniformly at random and a random binary mask $\mathbf{q}^t = (q_i^t)_{i \in \Omega^t} \in \mathbb{R}^{d \times c}$ generated as explained in Figure 1. The compressed vector $\mathcal{C}_i^t(v)$ is v multiplied elementwise by q_i^t .

2: **for** $t = 0, 1, \dots$ **do**

3: **for** $i = 1, \dots, n$, at clients in parallel, **do**

4: $\hat{x}_i^t := x_i^t - \gamma g_i^t + \gamma h_i^t$, where g_i^t is an unbiased stochastic estimate of $\nabla f_i(x_i^t)$ of variance σ_i^2

5: **if** $\theta^t = 1$ **then**

6: **if** $i \in \Omega^t$ **then**

7: send \hat{x}_i^t to the server, which aggregates $\bar{x}^t := \frac{1}{s} \sum_{j \in \Omega^t} \mathcal{C}_j^t(\hat{x}_j^t)$ and broadcasts it to all clients

8: $h_i^{t+1} := h_i^t + \frac{p\chi}{\gamma} (\mathcal{C}_i^t(\bar{x}^t) - \mathcal{C}_i^t(\hat{x}_i^t))$

9: **else**

10: $h_i^{t+1} := h_i^t$

11: **end if**

12: $x_i^{t+1} := \bar{x}^t$

13: **else**

14: $x_i^{t+1} := \hat{x}_i^t$

15: $h_i^{t+1} := h_i^t$

16: **end if**

17: **end for**

18: **end for**

Appendix

A Proof of Theorem 1

We first prove convergence of Algorithm 2, which is a single-loop version of **TAMUNA**; that is, there is a unique loop over the iterations and there is one local step per iteration. In Section A.2, we show that this yields a proof of Theorem 1 for **TAMUNA**. We can note that in case of full participation ($c = n$, $\Omega^t \equiv [n]$), Algorithm 2 reverts to **CompressedScaffnew** [Condat et al., 2022a].

To simplify the analysis of Algorithm 2, we introduce vector notations: the problem (1) can be written as

$$\text{find } \mathbf{x}^* = \arg \min_{\mathbf{x} \in \mathcal{X}} \mathbf{f}(\mathbf{x}) \quad \text{s.t.} \quad W\mathbf{x} = 0, \quad (21)$$

where $\mathcal{X} := \mathbb{R}^{d \times n}$, an element $\mathbf{x} = (x_i)_{i=1}^n \in \mathcal{X}$ is a collection of vectors $x_i \in \mathbb{R}^d$, $\mathbf{f} : \mathbf{x} \in \mathcal{X} \mapsto \sum_{i=1}^n f_i(x_i)$ is \mathcal{L} -smooth and μ -strongly convex, the linear operator $W : \mathcal{X} \rightarrow \mathcal{X}$ maps $\mathbf{x} = (x_i)_{i=1}^n$ to $(x_i - \frac{1}{n} \sum_{j=1}^n x_j)_{i=1}^n$. The constraint $W\mathbf{x} = 0$ means that \mathbf{x} minus its average is zero; that is, \mathbf{x} has identical components $x_1 = \dots = x_n$. Thus, (21) is indeed equivalent to (1). We have $W = W^* = W^2$.

We also rewrite Algorithm 2 using vector notations as Algorithm 3. It converges linearly:

Algorithm 3

input: stepsizes $\gamma > 0$, $\chi > 0$; probability $p \in (0, 1]$, parameter $\omega \geq 0$; number of participating clients $c \in \{2, \dots, n\}$; compression index $s \in \{2, \dots, c\}$; initial estimates $\mathbf{x}^0 \in \mathcal{X}$ and $\mathbf{h}^0 \in \mathcal{X}$ such that $\sum_{i=1}^n h_i^0 = 0$; sequence of independent coin flips $\theta^0, \theta^1, \dots$ with $\text{Prob}(\theta^t = 1) = p$, and for every t with $\theta^t = 1$, a subset $\Omega^t \subset [n]$ of size c chosen uniformly at random and a random binary mask $\mathbf{q}^t = (q_i^t)_{i \in \Omega^t} \in \mathbb{R}^{d \times c}$ generated as explained in Figure 1. The compressed vector $\mathcal{C}_i^t(v)$ is v multiplied elementwise by q_i^t .

for $t = 0, 1, \dots$ **do**

$$\hat{\mathbf{x}}^t := \mathbf{x}^t - \gamma \mathbf{g}^t + \gamma \mathbf{h}^t, \text{ where } \mathbf{g}^t = (g_i^t)_{i=1}^n \approx \nabla \mathbf{f}(\mathbf{x}^t)$$

if $\theta^t = 1$ **then**

$$\bar{\mathbf{x}}^t := (\bar{x}_i^t)_{i=1}^n, \text{ where } \bar{x}^t := \frac{1}{s} \sum_{j \in \Omega^t} \mathcal{C}_j^t(\hat{x}_j^t)$$

$$\mathbf{x}^{t+1} := \bar{\mathbf{x}}^t$$

$$\mathbf{d}^t := (d_i^t)_{i=1}^n \text{ with } d_i^t = \begin{cases} (1 + \omega) (\mathcal{C}_i^t(\hat{x}_i^t) - \mathcal{C}_i^t(\bar{x}_i^t)) & \text{if } i \in \Omega^t, \\ 0 & \text{otherwise} \end{cases}$$

else

$$\mathbf{x}^{t+1} := \hat{\mathbf{x}}^t$$

$$\mathbf{d}^t := 0$$

end if

$$\mathbf{h}^{t+1} := \mathbf{h}^t - \frac{p\chi}{\gamma(1+\omega)} \mathbf{d}^t$$

end for

Theorem 6 (fast linear convergence). *In Algorithm 3, suppose that $0 < \gamma < \frac{2}{\mathcal{L}}$, $0 < \chi \leq \frac{n(s-1)}{s(n-1)}$, $\omega = \frac{n-1}{p(s-1)} - 1$. For every $t \geq 0$, define the Lyapunov function*

$$\Psi^t := \frac{1}{\gamma} \|\mathbf{x}^t - \mathbf{x}^*\|^2 + \frac{\gamma(1+\omega)}{p\chi} \|\mathbf{h}^t - \mathbf{h}^*\|^2, \quad (22)$$

where \mathbf{x}^* is the unique solution to (21) and $\mathbf{h}^* := \nabla \mathbf{f}(\mathbf{x}^*)$. Then Algorithm 3 converges linearly: for every $t \geq 0$,

$$\mathbb{E}[\Psi^t] \leq \tau^t \Psi^0 + \frac{\gamma\sigma^2}{1-\tau}, \quad (23)$$

where

$$\tau := \max \left((1 - \gamma\mu)^2, (\gamma\mathcal{L} - 1)^2, 1 - p^2\chi \frac{s-1}{n-1} \right) < 1. \quad (24)$$

Also, if $\sigma = 0$, $(\mathbf{x}^t)_{t \in \mathbb{N}}$ and $(\hat{\mathbf{x}}^t)_{t \in \mathbb{N}}$ both converge to \mathbf{x}^* and $(\mathbf{h}^t)_{t \in \mathbb{N}}$ converges to \mathbf{h}^* , almost surely.

Proof. We consider the variables of Algorithm 3. For every $t \geq 0$, we denote by \mathcal{F}_0^t the σ -algebra generated by the collection of \mathcal{X} -valued random variables $\mathbf{x}^0, \mathbf{h}^0, \dots, \mathbf{x}^t, \mathbf{h}^t$, and by \mathcal{F}^t the σ -algebra generated by these variables, as well as the stochastic gradients \mathbf{g}^t . \mathbf{d}^t is a random variable; as proved in Section A.1, it satisfies the 3 following properties, on which the convergence analysis of Algorithm 3 relies: for every $t \geq 0$,

1. $\mathbb{E}[\mathbf{d}^t \mid \mathcal{F}^t] = W \hat{\mathbf{x}}^t$.
2. $\mathbb{E}[\|\mathbf{d}^t - W \hat{\mathbf{x}}^t\|^2 \mid \mathcal{F}^t] \leq \omega \|W \hat{\mathbf{x}}^t\|^2$.

3. \mathbf{d}^t belongs to the range of W ; that is, $\sum_{i=1}^n d_i^t = 0$.

We suppose that $\sum_{i=1}^n h_i^0 = 0$. Then, it follows from the third property of \mathbf{d}^t that, for every $t \geq 0$, $\sum_{i=1}^n h_i^t = 0$; that is, $W\mathbf{h}^t = \mathbf{h}^t$.

For every $t \geq 0$, we define $\hat{\mathbf{h}}^{t+1} := \mathbf{h}^t - \frac{p\chi}{\gamma}W\hat{\mathbf{x}}^t$, $\mathbf{w}^t := \mathbf{x}^t - \gamma\mathbf{g}^t$ and $\mathbf{w}^* := \mathbf{x}^* - \gamma\nabla\mathbf{f}(\mathbf{x}^*)$. We also define $\bar{\mathbf{x}}^{t\sharp} := (\bar{x}^{t\sharp})_{i=1}^n$, with $\bar{x}^{t\sharp} := \frac{1}{n}\sum_{i=1}^n \hat{x}_i^t$; that is, $\bar{x}^{t\sharp}$ is the exact average of the \hat{x}_i^t , of which \bar{x}^t is an unbiased random estimate.

Let $t \geq 0$. We have

$$\mathbb{E}\left[\|\mathbf{x}^{t+1} - \mathbf{x}^*\|^2 \mid \mathcal{F}^t\right] = p\mathbb{E}\left[\|\bar{\mathbf{x}}^t - \mathbf{x}^*\|^2 \mid \mathcal{F}^t, \theta^t = 1\right] + (1-p)\|\hat{\mathbf{x}}^t - \mathbf{x}^*\|^2,$$

Since $\mathbb{E}[\bar{\mathbf{x}}^t \mid \mathcal{F}^t, \theta^t = 1] = \bar{\mathbf{x}}^{t\sharp}$,

$$\mathbb{E}\left[\|\bar{\mathbf{x}}^t - \mathbf{x}^*\|^2 \mid \mathcal{F}^t, \theta^t = 1\right] = \|\bar{\mathbf{x}}^{t\sharp} - \mathbf{x}^*\|^2 + \mathbb{E}\left[\|\bar{\mathbf{x}}^t - \bar{\mathbf{x}}^{t\sharp}\|^2 \mid \mathcal{F}^t, \theta^t = 1\right],$$

with

$$\|\bar{\mathbf{x}}^{t\sharp} - \mathbf{x}^*\|^2 = \|\hat{\mathbf{x}}^t - \mathbf{x}^*\|^2 - \|W\hat{\mathbf{x}}^t\|^2.$$

To analyze $\mathbb{E}\left[\|\bar{\mathbf{x}}^t - \mathbf{x}^*\|^2 \mid \mathcal{F}^t, \theta^t = 1\right]$, where the expectation is with respect to the active subset Ω^t and the mask \mathbf{q}^t , we can remark that the expectation and the squared Euclidean norm are separable with respect to the coordinates of the d -dimensional vectors. So, we can reason on the coordinates independently on each other, even if the the coordinates, or rows, of \mathbf{q}^t are mutually dependent. Also, for a given coordinate $k \in [d]$, choosing s elements at random among the c elements $\hat{x}_{i,k}^t$ with $i \in \Omega^t$, with Ω^t chosen uniformly at random too, is equivalent to selecting s elements $\hat{x}_{i,k}^t$ among all $i \in [n]$ uniformly at random in the first place. Thus, for every coordinate $k \in [d]$, it is like a subset $\tilde{\Omega}_k^t \subset [n]$ of size s , which corresponds to the location of the ones in the k -th row of \mathbf{q}^t , is chosen uniformly at random and

$$\bar{x}_k^t = \frac{1}{s} \sum_{i \in \tilde{\Omega}_k^t} \hat{x}_{i,k}^t.$$

Then, as proved in Condat and Richtárik [2022, Proposition 1],

$$\mathbb{E}\left[\|\bar{\mathbf{x}}^t - \bar{\mathbf{x}}^{t\sharp}\|^2 \mid \mathcal{F}^t, \theta^t = 1\right] = n \sum_{k=1}^d \mathbb{E}_{\tilde{\Omega}_k^t} \left[\left(\frac{1}{s} \sum_{i \in \tilde{\Omega}_k^t} \hat{x}_{i,k}^t - \frac{1}{n} \sum_{j=1}^n \hat{x}_{j,k}^t \right)^2 \mid \mathcal{F}^t \right] = \nu \|W\hat{\mathbf{x}}^t\|^2,$$

where

$$\nu := \frac{n-s}{s(n-1)} \in \left[0, \frac{1}{2}\right). \quad (25)$$

Moreover,

$$\begin{aligned} \|\hat{\mathbf{x}}^t - \mathbf{x}^*\|^2 &= \|\mathbf{w}^t - \mathbf{w}^*\|^2 + \gamma^2 \|\mathbf{h}^t - \mathbf{h}^*\|^2 + 2\gamma \langle \mathbf{w}^t - \mathbf{w}^*, \mathbf{h}^t - \mathbf{h}^* \rangle \\ &= \|\mathbf{w}^t - \mathbf{w}^*\|^2 - \gamma^2 \|\mathbf{h}^t - \mathbf{h}^*\|^2 + 2\gamma \langle \hat{\mathbf{x}}^t - \mathbf{x}^*, \mathbf{h}^t - \mathbf{h}^* \rangle \\ &= \|\mathbf{w}^t - \mathbf{w}^*\|^2 - \gamma^2 \|\mathbf{h}^t - \mathbf{h}^*\|^2 + 2\gamma \langle \hat{\mathbf{x}}^t - \mathbf{x}^*, \hat{\mathbf{h}}^{t+1} - \mathbf{h}^* \rangle - 2\gamma \langle \hat{\mathbf{x}}^t - \mathbf{x}^*, \hat{\mathbf{h}}^{t+1} - \mathbf{h}^t \rangle \\ &= \|\mathbf{w}^t - \mathbf{w}^*\|^2 - \gamma^2 \|\mathbf{h}^t - \mathbf{h}^*\|^2 + 2\gamma \langle \hat{\mathbf{x}}^t - \mathbf{x}^*, \hat{\mathbf{h}}^{t+1} - \mathbf{h}^* \rangle + 2p\chi \langle \hat{\mathbf{x}}^t - \mathbf{x}^*, W\hat{\mathbf{x}}^t \rangle \\ &= \|\mathbf{w}^t - \mathbf{w}^*\|^2 - \gamma^2 \|\mathbf{h}^t - \mathbf{h}^*\|^2 + 2\gamma \langle \hat{\mathbf{x}}^t - \mathbf{x}^*, \hat{\mathbf{h}}^{t+1} - \mathbf{h}^* \rangle + 2p\chi \|W\hat{\mathbf{x}}^t\|^2. \end{aligned}$$

Hence,

$$\begin{aligned}
\mathbb{E}\left[\|\mathbf{x}^{t+1} - \mathbf{x}^*\|^2 \mid \mathcal{F}^t\right] &= p\|\hat{\mathbf{x}}^t - \mathbf{x}^*\|^2 - p\|W\hat{\mathbf{x}}^t\|^2 + p\nu\|W\hat{\mathbf{x}}^t\|^2 + (1-p)\|\hat{\mathbf{x}}^t - \mathbf{x}^*\|^2 \\
&= \|\hat{\mathbf{x}}^t - \mathbf{x}^*\|^2 - p(1-\nu)\|W\hat{\mathbf{x}}^t\|^2 \\
&= \|\mathbf{w}^t - \mathbf{w}^*\|^2 - \gamma^2\|\mathbf{h}^t - \mathbf{h}^*\|^2 + 2\gamma\langle\hat{\mathbf{x}}^t - \mathbf{x}^*, \hat{\mathbf{h}}^{t+1} - \mathbf{h}^*\rangle \\
&\quad + (2p\chi - p(1-\nu))\|W\hat{\mathbf{x}}^t\|^2.
\end{aligned}$$

On the other hand, using the 3 properties of \mathbf{d}^t stated above, we have

$$\begin{aligned}
\mathbb{E}\left[\|\mathbf{h}^{t+1} - \mathbf{h}^*\|^2 \mid \mathcal{F}^t\right] &\leq \left\|\mathbf{h}^t - \mathbf{h}^* - \frac{p\chi}{\gamma(1+\omega)}W\hat{\mathbf{x}}^t\right\|^2 + \frac{\omega p^2\chi^2}{\gamma^2(1+\omega)^2}\|W\hat{\mathbf{x}}^t\|^2 \\
&= \left\|\mathbf{h}^t - \mathbf{h}^* + \frac{1}{1+\omega}(\hat{\mathbf{h}}^{t+1} - \mathbf{h}^t)\right\|^2 + \frac{\omega}{(1+\omega)^2}\|\hat{\mathbf{h}}^{t+1} - \mathbf{h}^t\|^2 \\
&= \left\|\frac{\omega}{1+\omega}(\mathbf{h}^t - \mathbf{h}^*) + \frac{1}{1+\omega}(\hat{\mathbf{h}}^{t+1} - \mathbf{h}^*)\right\|^2 + \frac{\omega}{(1+\omega)^2}\|\hat{\mathbf{h}}^{t+1} - \mathbf{h}^t\|^2 \\
&= \frac{\omega^2}{(1+\omega)^2}\|\mathbf{h}^t - \mathbf{h}^*\|^2 + \frac{1}{(1+\omega)^2}\|\hat{\mathbf{h}}^{t+1} - \mathbf{h}^*\|^2 \\
&\quad + \frac{2\omega}{(1+\omega)^2}\langle\mathbf{h}^t - \mathbf{h}^*, \hat{\mathbf{h}}^{t+1} - \mathbf{h}^*\rangle + \frac{\omega}{(1+\omega)^2}\|\hat{\mathbf{h}}^{t+1} - \mathbf{h}^*\|^2 \\
&\quad + \frac{\omega}{(1+\omega)^2}\|\mathbf{h}^t - \mathbf{h}^*\|^2 - \frac{2\omega}{(1+\omega)^2}\langle\mathbf{h}^t - \mathbf{h}^*, \hat{\mathbf{h}}^{t+1} - \mathbf{h}^*\rangle \\
&= \frac{1}{1+\omega}\|\hat{\mathbf{h}}^{t+1} - \mathbf{h}^*\|^2 + \frac{\omega}{1+\omega}\|\mathbf{h}^t - \mathbf{h}^*\|^2.
\end{aligned}$$

Moreover,

$$\begin{aligned}
\|\hat{\mathbf{h}}^{t+1} - \mathbf{h}^*\|^2 &= \|(\mathbf{h}^t - \mathbf{h}^*) + (\hat{\mathbf{h}}^{t+1} - \mathbf{h}^t)\|^2 \\
&= \|\mathbf{h}^t - \mathbf{h}^*\|^2 + \|\hat{\mathbf{h}}^{t+1} - \mathbf{h}^t\|^2 + 2\langle\mathbf{h}^t - \mathbf{h}^*, \hat{\mathbf{h}}^{t+1} - \mathbf{h}^t\rangle \\
&= \|\mathbf{h}^t - \mathbf{h}^*\|^2 + 2\langle\hat{\mathbf{h}}^{t+1} - \mathbf{h}^*, \hat{\mathbf{h}}^{t+1} - \mathbf{h}^t\rangle - \|\hat{\mathbf{h}}^{t+1} - \mathbf{h}^t\|^2 \\
&= \|\mathbf{h}^t - \mathbf{h}^*\|^2 - \|\hat{\mathbf{h}}^{t+1} - \mathbf{h}^t\|^2 - 2\frac{p\chi}{\gamma}\langle\hat{\mathbf{h}}^{t+1} - \mathbf{h}^*, W(\hat{\mathbf{x}}^t - \mathbf{x}^*)\rangle \\
&= \|\mathbf{h}^t - \mathbf{h}^*\|^2 - \frac{p^2\chi^2}{\gamma^2}\|W\hat{\mathbf{x}}^t\|^2 - 2\frac{p\chi}{\gamma}\langle W(\hat{\mathbf{h}}^{t+1} - \mathbf{h}^*), \hat{\mathbf{x}}^t - \mathbf{x}^*\rangle \\
&= \|\mathbf{h}^t - \mathbf{h}^*\|^2 - \frac{p^2\chi^2}{\gamma^2}\|W\hat{\mathbf{x}}^t\|^2 - 2\frac{p\chi}{\gamma}\langle\hat{\mathbf{h}}^{t+1} - \mathbf{h}^*, \hat{\mathbf{x}}^t - \mathbf{x}^*\rangle.
\end{aligned}$$

Hence,

$$\begin{aligned}
& \frac{1}{\gamma} \mathbb{E} \left[\|\mathbf{x}^{t+1} - \mathbf{x}^*\|^2 \mid \mathcal{F}^t \right] + \frac{\gamma(1+\omega)}{p\chi} \mathbb{E} \left[\|\mathbf{h}^{t+1} - \mathbf{h}^*\|^2 \mid \mathcal{F}^t \right] \\
& \leq \frac{1}{\gamma} \|\mathbf{w}^t - \mathbf{w}^*\|^2 - \gamma \|\mathbf{h}^t - \mathbf{h}^*\|^2 + \left(2\frac{p\chi}{\gamma} - \frac{p}{\gamma}(1-\nu) \right) \|W\hat{\mathbf{x}}^t\|^2 \\
& \quad + 2\langle \hat{\mathbf{x}}^t - \mathbf{x}^*, \hat{\mathbf{h}}^{t+1} - \mathbf{h}^* \rangle + \frac{\gamma}{p\chi} \|\mathbf{h}^t - \mathbf{h}^*\|^2 \\
& \quad - \frac{p\chi}{\gamma} \|W\hat{\mathbf{x}}^t\|^2 - 2\langle \hat{\mathbf{h}}^{t+1} - \mathbf{h}^*, \hat{\mathbf{x}}^t - \mathbf{x}^* \rangle + \frac{\gamma\omega}{p\chi} \|\mathbf{h}^t - \mathbf{h}^*\|^2 \\
& = \frac{1}{\gamma} \|\mathbf{w}^t - \mathbf{w}^*\|^2 + \left(\frac{\gamma(1+\omega)}{p\chi} - \gamma \right) \|\mathbf{h}^t - \mathbf{h}^*\|^2 \\
& \quad + \left(\frac{p\chi}{\gamma} - \frac{p(1-\nu)}{\gamma} \right) \|W\hat{\mathbf{x}}^t\|^2. \tag{26}
\end{aligned}$$

Since we have supposed

$$0 < \chi \leq 1 - \nu = \frac{n(s-1)}{s(n-1)} \in \left(\frac{1}{2}, 1 \right],$$

we have

$$\begin{aligned}
& \frac{1}{\gamma} \mathbb{E} \left[\|\mathbf{x}^{t+1} - \mathbf{x}^*\|^2 \mid \mathcal{F}^t \right] + \frac{\gamma(1+\omega)}{p\chi} \mathbb{E} \left[\|\mathbf{h}^{t+1} - \mathbf{h}^*\|^2 \mid \mathcal{F}^t \right] \\
& \leq \frac{1}{\gamma} \|\mathbf{w}^t - \mathbf{w}^*\|^2 + \frac{\gamma(1+\omega)}{p\chi} \left(1 - \frac{p\chi}{1+\omega} \right) \|\mathbf{h}^t - \mathbf{h}^*\|^2.
\end{aligned}$$

Finally,

$$\mathbb{E} \left[\|\mathbf{w}^t - \mathbf{w}^*\|^2 \mid \mathcal{F}_0^t \right] \leq \|(\text{Id} - \gamma\nabla\mathbf{f})\mathbf{x}^t - (\text{Id} - \gamma\nabla\mathbf{f})\mathbf{x}^*\|^2 + \gamma^2\sigma^2,$$

and according to Condat and Richtárik [2023, Lemma 1],

$$\|(\text{Id} - \gamma\nabla\mathbf{f})\mathbf{x}^t - (\text{Id} - \gamma\nabla\mathbf{f})\mathbf{x}^*\|^2 \leq \max(1 - \gamma\mu, \gamma\mathcal{L} - 1)^2 \|\mathbf{x}^t - \mathbf{x}^*\|^2.$$

Therefore,

$$\begin{aligned}
\mathbb{E} \left[\Psi^{t+1} \mid \mathcal{F}_0^t \right] & \leq \max \left((1 - \gamma\mu)^2, (\gamma\mathcal{L} - 1)^2, 1 - \frac{p\chi}{1+\omega} \right) \Psi^t + \gamma\sigma^2 \\
& = \max \left((1 - \gamma\mu)^2, (\gamma\mathcal{L} - 1)^2, 1 - p^2\chi \frac{s-1}{n-1} \right) \Psi^t + \gamma\sigma^2. \tag{27}
\end{aligned}$$

Using the tower rule, we can unroll the recursion in (27) to obtain the unconditional expectation of Ψ^{t+1} .

If $\sigma = 0$, using classical results on supermartingale convergence [Bertsekas, 2015, Proposition A.4.5], it follows from (27) that $\Psi^t \rightarrow 0$ almost surely. Almost sure convergence of \mathbf{x}^t and \mathbf{h}^t follows. Finally, by Lipschitz continuity of $\nabla\mathbf{f}$, we can upper bound $\|\hat{\mathbf{x}}^t - \mathbf{x}^*\|^2$ by a linear combination of $\|\mathbf{x}^t - \mathbf{x}^*\|^2$ and $\|\mathbf{h}^t - \mathbf{h}^*\|^2$. It follows that $\mathbb{E} \left[\|\hat{\mathbf{x}}^t - \mathbf{x}^*\|^2 \right] \rightarrow 0$ linearly with the same rate τ and that $\hat{\mathbf{x}}^t \rightarrow \mathbf{x}^*$ almost surely, as well. \square

A.1 The Random Variable \mathbf{d}^t

We study the random variable \mathbf{d}^t used in Algorithm 3. If $\theta^t = 0$, $\mathbf{d}^t = 0$. If, on the other hand, $\theta^t = 1$, for every coordinate $k \in [d]$, a subset $\tilde{\Omega}_k^t \subset [n]$ of size s is chosen uniformly at random. These sets $(\tilde{\Omega}_k^t)_{k=1}^d$ are mutually dependent, but this does not matter for the derivations, since we can reason on the coordinates separately. Then, for every $k \in [d]$ and $i \in [n]$,

$$d_{i,k}^t := \begin{cases} a \left(\hat{x}_{i,k}^t - \frac{1}{s} \sum_{j \in \tilde{\Omega}_k^t} \hat{x}_{j,k}^t \right) & \text{if } i \in \tilde{\Omega}_k^t, \\ 0 & \text{otherwise,} \end{cases} \quad (28)$$

for some value $a > 0$ to determine. We can check that $\sum_{i=1}^n d_i^t = 0$. We can also note that \mathbf{d}^t depends only on $W\hat{\mathbf{x}}^t$ and not on $\hat{\mathbf{x}}^t$; in particular, if $\hat{x}_1^t = \dots = \hat{x}_n^t$, $d_i^t = 0$. We have to set a so that $\mathbb{E}[d_i^t] = \hat{x}_i^t - \frac{1}{n} \sum_{j=1}^n \hat{x}_j^t$, where the expectation is with respect to θ^t and the $\tilde{\Omega}_k^t$ (all expectations in this section are conditional to $\hat{\mathbf{x}}^t$). So, let us calculate this expectation.

Let $k \in [d]$. For every $i \in [n]$,

$$\mathbb{E}[d_{i,k}^t] = p \frac{s}{n} \left(a \hat{x}_{i,k}^t - \frac{a}{s} \mathbb{E}_{\Omega:i \in \Omega} \left[\sum_{j \in \Omega} \hat{x}_{j,k}^t \right] \right),$$

where $\mathbb{E}_{\Omega:i \in \Omega}$ denotes the expectation with respect to a subset $\Omega \subset [n]$ of size s containing i and chosen uniformly at random. We have

$$\mathbb{E}_{\Omega:i \in \Omega} \left[\sum_{j \in \Omega} \hat{x}_{j,k}^t \right] = \hat{x}_{i,k}^t + \frac{s-1}{n-1} \sum_{j \in [n] \setminus \{i\}} \hat{x}_{j,k}^t = \frac{n-s}{n-1} \hat{x}_{i,k}^t + \frac{s-1}{n-1} \sum_{j=1}^n \hat{x}_{j,k}^t.$$

Hence, for every $i \in [n]$,

$$\mathbb{E}[d_{i,k}^t] = p \frac{s}{n} \left(a - \frac{a(n-s)}{s(n-1)} \right) \hat{x}_{i,k}^t - p \frac{s}{n} \frac{a(s-1)}{s(n-1)} \sum_{j=1}^n \hat{x}_{j,k}^t.$$

Therefore, by setting

$$a := \frac{n-1}{p(s-1)}, \quad (29)$$

we have, for every $i \in [n]$,

$$\begin{aligned} \mathbb{E}[d_{i,k}^t] &= p \frac{s}{n} \left(\frac{1}{p} \frac{n-1}{s-1} - \frac{1}{p} \frac{n-s}{s(s-1)} \right) \hat{x}_{i,k}^t - \frac{1}{n} \sum_{j=1}^n \hat{x}_{j,k}^t \\ &= \hat{x}_{i,k}^t - \frac{1}{n} \sum_{j=1}^n \hat{x}_{j,k}^t, \end{aligned}$$

as desired.

Now, we want to find the value of ω such that

$$\mathbb{E} \left[\|\mathbf{d}^t - W\hat{\mathbf{x}}^t\|^2 \right] \leq \omega \|W\hat{\mathbf{x}}^t\|^2 \quad (30)$$

or, equivalently,

$$\mathbb{E} \left[\sum_{i=1}^n \|d_i^t\|^2 \right] \leq (1 + \omega) \sum_{i=1}^n \left\| \hat{x}_i^t - \frac{1}{n} \sum_{j=1}^n \hat{x}_j^t \right\|^2.$$

We can reason on the coordinates separately, or all at once to ease the notations. We have

$$\mathbb{E} \left[\sum_{i=1}^n \|d_i^t\|^2 \right] = p \frac{s}{n} \sum_{i=1}^n \mathbb{E}_{\Omega: i \in \Omega} \left\| a \hat{x}_i^t - \frac{a}{s} \sum_{j \in \Omega} \hat{x}_j^t \right\|^2.$$

For every $i \in [n]$,

$$\begin{aligned} \mathbb{E}_{\Omega: i \in \Omega} \left\| a \hat{x}_i^t - \frac{a}{s} \sum_{j \in \Omega} \hat{x}_j^t \right\|^2 &= \mathbb{E}_{\Omega: i \in \Omega} \left\| \left(a - \frac{a}{s} \right) \hat{x}_i^t - \frac{a}{s} \sum_{j \in \Omega \setminus \{i\}} \hat{x}_j^t \right\|^2 \\ &= \left\| \left(a - \frac{a}{s} \right) \hat{x}_i^t \right\|^2 + \mathbb{E}_{\Omega: i \in \Omega} \left\| \frac{a}{s} \sum_{j \in \Omega \setminus \{i\}} \hat{x}_j^t \right\|^2 \\ &\quad - 2 \left\langle \left(a - \frac{a}{s} \right) \hat{x}_i^t, \frac{a}{s} \mathbb{E}_{\Omega: i \in \Omega} \sum_{j \in \Omega \setminus \{i\}} \hat{x}_j^t \right\rangle. \end{aligned}$$

We have

$$\mathbb{E}_{\Omega: i \in \Omega} \sum_{j \in \Omega \setminus \{i\}} \hat{x}_j^t = \frac{s-1}{n-1} \sum_{j \in [n] \setminus \{i\}} \hat{x}_j^t = \frac{s-1}{n-1} \left(\sum_{j=1}^n \hat{x}_j^t - \hat{x}_i^t \right)$$

and

$$\begin{aligned} \mathbb{E}_{\Omega: i \in \Omega} \left\| \sum_{j \in \Omega \setminus \{i\}} \hat{x}_j^t \right\|^2 &= \mathbb{E}_{\Omega: i \in \Omega} \sum_{j \in \Omega \setminus \{i\}} \|\hat{x}_j^t\|^2 + \mathbb{E}_{\Omega: i \in \Omega} \sum_{j \in \Omega \setminus \{i\}} \sum_{j' \in \Omega \setminus \{i, j\}} \langle \hat{x}_j^t, \hat{x}_{j'}^t \rangle \\ &= \frac{s-1}{n-1} \sum_{j \in [n] \setminus \{i\}} \|\hat{x}_j^t\|^2 + \frac{s-1}{n-1} \frac{s-2}{n-2} \sum_{j \in [n] \setminus \{i\}} \sum_{j' \in [n] \setminus \{i, j\}} \langle \hat{x}_j^t, \hat{x}_{j'}^t \rangle \\ &= \frac{s-1}{n-1} \left(1 - \frac{s-2}{n-2} \right) \sum_{j \in [n] \setminus \{i\}} \|\hat{x}_j^t\|^2 + \frac{s-1}{n-1} \frac{s-2}{n-2} \left\| \sum_{j \in [n] \setminus \{i\}} \hat{x}_j^t \right\|^2 \\ &= \frac{s-1}{n-1} \frac{n-s}{n-2} \left(\sum_{j=1}^n \|\hat{x}_j^t\|^2 - \|\hat{x}_i^t\|^2 \right) + \frac{s-1}{n-1} \frac{s-2}{n-2} \left\| \sum_{j=1}^n \hat{x}_j^t - \hat{x}_i^t \right\|^2. \end{aligned}$$

Hence,

$$\begin{aligned}
\mathbb{E} \left[\sum_{i=1}^n \|d_i^t\|^2 \right] &= p \frac{s}{n} \sum_{i=1}^n \left\| \left(a - \frac{a}{s} \right) \hat{x}_i^t \right\|^2 + ps \frac{a^2}{(s)^2} \frac{s-1}{n-1} \frac{n-s}{n-2} \sum_{j=1}^n \|\hat{x}_j^t\|^2 \\
&\quad - p \frac{s}{n} \frac{a^2}{(s)^2} \frac{s-1}{n-1} \frac{n-s}{n-2} \sum_{i=1}^n \|\hat{x}_i^t\|^2 + p \frac{s}{n} \frac{a^2}{(s)^2} \frac{s-1}{n-1} \frac{s-2}{n-2} \sum_{i=1}^n \left\| \sum_{j=1}^n \hat{x}_j^t - \hat{x}_i^t \right\|^2 \\
&\quad - 2p \frac{s}{n} \frac{a}{s} \frac{s-1}{n-1} \left(a - \frac{a}{s} \right) \sum_{i=1}^n \left\langle \hat{x}_i^t, \sum_{j=1}^n \hat{x}_j^t - \hat{x}_i^t \right\rangle \\
&= \frac{(n-1)^2}{psn} \sum_{i=1}^n \|\hat{x}_i^t\|^2 + \frac{(n-1)^2}{ps(s-1)n} \frac{n-s}{n-2} \sum_{i=1}^n \|\hat{x}_i^t\|^2 \\
&\quad + \frac{1}{ps} \frac{s-2}{s-1} \frac{n-1}{n-2} \left\| \sum_{i=1}^n \hat{x}_i^t \right\|^2 - 2 \frac{1}{psn} \frac{s-2}{s-1} \frac{n-1}{n-2} \left\| \sum_{i=1}^n \hat{x}_i^t \right\|^2 \\
&\quad + \frac{1}{psn} \frac{s-2}{s-1} \frac{n-1}{n-2} \sum_{i=1}^n \|\hat{x}_i^t\|^2 + 2 \frac{n-1}{psn} \sum_{i=1}^n \|\hat{x}_i^t\|^2 - 2 \frac{n-1}{psn} \left\| \sum_{i=1}^n \hat{x}_i^t \right\|^2 \\
&= \frac{(n-1)(n+1)}{psn} \sum_{i=1}^n \|\hat{x}_i^t\|^2 + \frac{(n-1)^2}{ps(s-1)n} \frac{n-s}{n-2} \sum_{i=1}^n \|\hat{x}_i^t\|^2 \\
&\quad - \frac{n-1}{psn} \frac{s}{s-1} \left\| \sum_{i=1}^n \hat{x}_i^t \right\|^2 + \frac{1}{psn} \frac{s-2}{s-1} \frac{n-1}{n-2} \sum_{i=1}^n \|\hat{x}_i^t\|^2 \\
&= \frac{(n^2-1)(s-1)(n-2) + (n-1)^2(n-s) + (s-2)(n-1)}{ps(s-1)n(n-2)} \sum_{i=1}^n \|\hat{x}_i^t\|^2 \\
&\quad - \frac{n-1}{p(s-1)n} \left\| \sum_{i=1}^n \hat{x}_i^t \right\|^2 \\
&= \frac{n-1}{p(s-1)} \sum_{i=1}^n \|\hat{x}_i^t\|^2 - \frac{n-1}{p(s-1)n} \left\| \sum_{i=1}^n \hat{x}_i^t \right\|^2 \\
&= \frac{n-1}{p(s-1)} \sum_{i=1}^n \left\| \hat{x}_i^t - \frac{1}{n} \sum_{j=1}^n \hat{x}_j^t \right\|^2.
\end{aligned}$$

Therefore, (30) holds with

$$\omega = \frac{n-1}{p(s-1)} - 1 \tag{31}$$

and we have $a = 1 + \omega$.

A.2 From Algorithm 2 to TAMUNA

TAMUNA is a two-loop version of Algorithm 2, where every sequence of local steps followed by a communication step is grouped into a round. One crucial observation about Algorithm 2 is the

following: for a client $i \notin \Omega^t$, which does not participate in communication at iteration t with $\theta^t = 1$, its variable x_i gets overwritten by \bar{x}^t anyway (step 12 of Algorithm 2). Therefore, all local steps it performed since its last participation are useless and can be omitted. But at iteration t with $\theta^t = 0$, it is still undecided whether or not a given client will participate in the next communication step at iteration $t' > t$, since $\Omega^{t'}$ has not yet been generated. That is why **TAMUNA** is written with two loops, so that it is decided at the beginning of the round which clients will communicate at the end of the round. Accordingly, at the beginning of round r , a client downloads the current model estimate (step 6 of **TAMUNA**) only if it participates ($i \in \Omega^{(r)}$), to initialize its sequence of local steps. Otherwise ($i \notin \Omega^{(r)}$), the client is completely idle: neither computation nor downlink or uplink communication is performed in round r . Finally, a round consists of a sequence of successive iterations with $\theta^t = 0$ and a last iteration with $\theta^t = 1$ followed by communication. Thus, the number of iterations, or local steps, in a round can be determined directly at the beginning of the round, according to a geometric law. Given these considerations, Algorithm 2 and **TAMUNA** are equivalent. In **TAMUNA**, the round and local step indexing is denoted by parentheses, e.g. (r, ℓ) , to differentiate it clearly from the iteration indexing.

To obtain Theorem 1 from Theorem 6, we first have to reindex the local steps to make the equivalent iteration index t in Algorithm 2 appear, since the rate is with respect to the number of iterations, not rounds, whose size is random. The almost sure convergence statement follows directly from the one in Theorem 6.

Importantly, we want a result related to the variables which are actually computed in **TAMUNA**, without including virtual variables by the idle clients, which are computed in Algorithm 2 but not in **TAMUNA**. That is why we express the convergence result with respect to \bar{x}^t , which relates only to the variables of active clients; also, \bar{x}^t is the model estimate known by the server whenever communication occurs, which matters at the end. Note the bar in $\bar{\Psi}$ in (6) to differentiate it from Ψ in (22). Thus, we continue the analysis of Algorithms 2 and 3 in Section A, with same definitions and notations. Let $t \geq 0$. If $\theta^t = 0$, we choose $\Omega^t \subset [n]$ of size c uniformly at random and a random binary mask $\mathbf{q}^t = (q_i^t)_{i \in \Omega^t} \in \mathbb{R}^{d \times c}$, and we define $\bar{x}^t := \frac{1}{s} \sum_{j \in \Omega^t} \mathcal{C}_j^t(\hat{x}_j^t)$ (in Theorem 1, for simplicity, Ω^t and \mathbf{q}^t are the ones that will be used at the end of the round; this choice is valid as it does not depend on the past). Ω^t , \mathbf{q}^t and \bar{x}^t are already defined if $\theta^t = 1$. We want to study $\mathbb{E} \left[\|\bar{x}^t - x^*\|^2 \mid \mathcal{F}^t \right]$, where the expectation is with respect to Ω^t and \mathbf{q}^t , whatever θ^t . Using the derivations already obtained,

$$\begin{aligned}
n \mathbb{E} \left[\|\bar{x}^t - x^*\|^2 \mid \mathcal{F}^t \right] &= \|\hat{\mathbf{x}}^t - \mathbf{x}^*\|^2 - \|W \hat{\mathbf{x}}^t\|^2 + \nu \|W \hat{\mathbf{x}}^t\|^2 \\
&= \|\mathbf{w}^t - \mathbf{w}^*\|^2 - \gamma^2 \|\mathbf{h}^t - \mathbf{h}^*\|^2 + 2\gamma \langle \hat{\mathbf{x}}^t - \mathbf{x}^*, \hat{\mathbf{h}}^{t+1} - \mathbf{h}^* \rangle \\
&\quad + (2p\chi + \nu - 1) \|W \hat{\mathbf{x}}^t\|^2 \\
&\leq \|\mathbf{w}^t - \mathbf{w}^*\|^2 - \gamma^2 \|\mathbf{h}^t - \mathbf{h}^*\|^2 + 2\gamma \langle \hat{\mathbf{x}}^t - \mathbf{x}^*, \hat{\mathbf{h}}^{t+1} - \mathbf{h}^* \rangle \\
&\quad + (2p\chi - p(1 - \nu)) \|W \hat{\mathbf{x}}^t\|^2.
\end{aligned}$$

Hence,

$$\begin{aligned}
\frac{n}{\gamma} \mathbb{E} \left[\|\bar{x}^t - x^*\|^2 \mid \mathcal{F}^t \right] &+ \frac{\gamma(1 + \omega)}{p\chi} \mathbb{E} \left[\|\mathbf{h}^{t+1} - \mathbf{h}^*\|^2 \mid \mathcal{F}^t \right] \\
&\leq \frac{1}{\gamma} \|\mathbf{w}^t - \mathbf{w}^*\|^2 + \frac{\gamma(1 + \omega)}{p\chi} \left(1 - \frac{p\chi}{1 + \omega} \right) \|\mathbf{h}^t - \mathbf{h}^*\|^2
\end{aligned}$$

and

$$\begin{aligned} & \frac{n}{\gamma} \mathbb{E} \left[\|\bar{x}^t - x^*\|^2 \mid \mathcal{F}_0^t \right] + \frac{\gamma(1+\omega)}{p\chi} \mathbb{E} \left[\|\mathbf{h}^{t+1} - \mathbf{h}^*\|^2 \mid \mathcal{F}_0^t \right] \\ & \leq \max \left((1-\gamma\mu)^2, (\gamma\mathcal{L}-1)^2, 1-p^2\chi \frac{s-1}{n-1} \right) \Psi^t + \gamma\sigma^2. \end{aligned}$$

Using the tower rule,

$$\frac{n}{\gamma} \mathbb{E} \left[\|\bar{x}^t - x^*\|^2 \right] + \frac{\gamma(1+\omega)}{p\chi} \mathbb{E} \left[\|\mathbf{h}^{t+1} - \mathbf{h}^*\|^2 \right] \leq \tau^t \Psi^0 + \frac{\gamma\sigma^2}{1-\tau}.$$

Since in **TAMUNA**, $x_1^0 = \dots = x_n^0 = \bar{x}^0 = \bar{x}^{(0)}$, $\bar{\Psi}^0 = \Psi^0$. This concludes the proof of Theorem 1.

B Proof of Theorem 3

We suppose that the assumptions in Theorem 3 hold. s is set as the maximum of three values. Let us consider these three cases.

1) Suppose that $s = 2$. Since $2 = s \geq \lfloor \alpha c \rfloor$ and $2 = s \geq \lfloor \frac{c}{d} \rfloor$, we have $\alpha \leq \frac{3}{c}$ and $1 \leq \frac{3d}{c}$. Hence,

$$\begin{aligned} & \mathcal{O} \left(\sqrt{\frac{n\kappa}{s}} + \frac{n}{s} \right) \left(\frac{sd}{c} + 1 + \alpha d \right) \\ & = \mathcal{O} \left(\sqrt{n\kappa} + n \right) \left(\frac{d}{c} + \frac{d}{c} + \frac{d}{c} \right) \\ & = \mathcal{O} \left(d \frac{\sqrt{n\kappa}}{c} + d \frac{n}{c} \right). \end{aligned} \tag{32}$$

2) Suppose that $s = \lfloor \frac{c}{d} \rfloor$. Then $\frac{sd}{c} \leq 1$. Since $s \geq \lfloor \alpha c \rfloor$ and $\lfloor \frac{c}{d} \rfloor = s \geq 2$, we have $\alpha c \leq s + 1 \leq \frac{c}{d} + 1$ and $\frac{d}{c} \leq \frac{1}{2}$, so that $\alpha d \leq 1 + \frac{d}{c} \leq 2$. Hence,

$$\begin{aligned} & \mathcal{O} \left(\sqrt{\frac{n\kappa}{s}} + \frac{n}{s} \right) \left(\frac{sd}{c} + 1 + \alpha d \right) \\ & = \mathcal{O} \left(\sqrt{\frac{n\kappa}{s}} + \frac{n}{s} \right). \end{aligned}$$

Since $2s \geq \frac{c}{d}$, we have $\frac{1}{s} \leq \frac{2d}{c}$ and

$$\begin{aligned} & \mathcal{O} \left(\sqrt{\frac{n\kappa}{s}} + \frac{n}{s} \right) \left(\frac{sd}{c} + 1 + \alpha d \right) \\ & = \mathcal{O} \left(\sqrt{d} \sqrt{\frac{n\kappa}{c}} + d \frac{n}{c} \right). \end{aligned} \tag{33}$$

3) Suppose that $s = \lfloor \alpha c \rfloor$. This implies $\alpha > 0$. Then $s \leq \alpha c$. Also, $2s \geq \alpha c$ and $\frac{1}{s} \leq \frac{2}{\alpha c}$. Since $s = \lfloor \alpha c \rfloor \geq \lfloor \frac{c}{d} \rfloor$, we have $\alpha c + 1 \geq \frac{c}{d}$ and $1 \leq \alpha d + \frac{d}{c}$. Since $s = \lfloor \alpha c \rfloor \geq 2$, we have $\frac{1}{c} \leq \frac{\alpha}{2}$ and

$1 \leq 2\alpha d$. Hence,

$$\begin{aligned}
& \mathcal{O}\left(\sqrt{\frac{n\kappa}{s}} + \frac{n}{s}\right)\left(\frac{sd}{c} + 1 + \alpha d\right) \\
&= \mathcal{O}\left(\sqrt{\frac{n\kappa}{\alpha c}} + \frac{n}{\alpha c}\right)(\alpha d + \alpha d + \alpha d) \\
&= \mathcal{O}\left(\sqrt{\alpha d}\sqrt{\frac{n\kappa}{c}} + d\frac{n}{c}\right). \tag{34}
\end{aligned}$$

By adding up the three upper bounds (32), (33), (34), we obtain the upper bound in (15).

C Sublinear Convergence in the Convex Case

In this section only, we remove the hypothesis of strong convexity: the functions f_i are only assumed to be convex and \mathcal{L} -smooth, and we suppose that a solution $x^* \in \mathbb{R}^d$ to (1) exists. Also, for simplicity, we only consider the case of exact gradients ($\sigma = 0$). Then we have sublinear ergodic convergence:

Theorem 7 (sublinear convergence). *In Algorithm 2 suppose that $\sigma = 0$ and that*

$$0 < \gamma < \frac{2}{\mathcal{L}} \quad \text{and} \quad 0 < \chi < \frac{n(s-1)}{s(n-1)} \in \left(\frac{1}{2}, 1\right]. \tag{35}$$

For every $i = 1, \dots, n$ and $T \geq 0$, let

$$\tilde{x}_i^T := \frac{1}{T+1} \sum_{t=0}^T x_i^t. \tag{36}$$

Then

$$\mathbb{E}\left[\|\nabla f(\tilde{x}_i^T)\|^2\right] = \mathcal{O}\left(\frac{1}{T}\right). \tag{37}$$

Proof. A solution $x^* \in \mathbb{R}^d$ to (1), which is supposed to exist, satisfies $\nabla f(x^*) = \frac{1}{n} \sum_{i=1}^n \nabla f_i(x^*) = 0$. x^* is not necessarily unique but $h_i^* := \nabla f_i(x^*)$ is unique.

We define the Bregman divergence of a \mathcal{L} -smooth convex function g at points $x, x' \in \mathbb{R}^d$ as $D_g(x, x') := g(x) - g(x') - \langle \nabla g(x'), x - x' \rangle \geq 0$. We have $D_g(x, x') \geq \frac{1}{2\mathcal{L}} \|\nabla g(x) - \nabla g(x')\|^2$. We note that for every $x \in \mathbb{R}^d$ and $i = 1, \dots, n$, $D_{f_i}(x, x^*)$ is the same whatever the solution x^* .

For every $t \geq 0$, we define the Lyapunov function

$$\Psi^t := \frac{1}{\gamma} \sum_{i=1}^n \|x_i^t - x^*\|^2 + \frac{\gamma}{p^2\chi} \frac{n-1}{s-1} \sum_{i=1}^n \|h_i^t - h_i^*\|^2, \tag{38}$$

Starting from (26), we have, for every $t \geq 0$,

$$\begin{aligned}
\mathbb{E}[\Psi^{t+1} \mid \mathcal{F}^t] &= \frac{1}{\gamma} \sum_{i=1}^n \mathbb{E}\left[\|x_i^{t+1} - x^*\|^2 \mid \mathcal{F}^t\right] + \frac{\gamma}{p^2\chi} \frac{n-1}{s-1} \sum_{i=1}^n \mathbb{E}\left[\|h_i^{t+1} - h_i^*\|^2 \mid \mathcal{F}^t\right] \\
&\leq \frac{1}{\gamma} \sum_{i=1}^n \|(x_i^t - \gamma \nabla f_i(x_i^t)) - (x^* - \gamma \nabla f_i(x^*))\|^2 \\
&\quad + \left(\frac{\gamma}{p^2\chi} \frac{n-1}{s-1} - \gamma\right) \sum_{i=1}^n \|h_i^t - h_i^*\|^2 + \frac{p}{\gamma} (\chi - 1 + \nu) \sum_{i=1}^n \left\| \hat{x}_i^t - \frac{1}{n} \sum_{j=1}^n \hat{x}_j^t \right\|^2,
\end{aligned}$$

with

$$\begin{aligned} \|(x_i^t - \gamma \nabla f_i(x_i^t)) - (x^* - \gamma \nabla f_i(x^*))\|^2 &= \|x_i^t - x^*\|^2 - 2\gamma \langle \nabla f_i(x_i^t) - \nabla f_i(x^*), x_i^t - x^* \rangle \\ &\quad + \gamma^2 \|\nabla f_i(x_i^t) - \nabla f_i(x^*)\|^2 \\ &\leq \|x_i^t - x^*\|^2 - (2\gamma - \gamma^2 \mathcal{L}) \langle \nabla f_i(x_i^t) - \nabla f_i(x^*), x_i^t - x^* \rangle, \end{aligned}$$

where the second inequality follows from cocoercivity of the gradient. Moreover, for every x, x' , $D_{f_i}(x, x') \leq \langle \nabla f_i(x) - \nabla f_i(x'), x - x' \rangle$. Therefore,

$$\begin{aligned} \mathbb{E}[\Psi^{t+1} | \mathcal{F}^t] &\leq \Psi^t - (2 - \gamma \mathcal{L}) \sum_{i=1}^n D_{f_i}(x_i^t, x^*) \\ &\quad - \gamma \sum_{i=1}^n \|h_i^t - h_i^*\|^2 + \frac{\rho}{\gamma} (\chi - 1 + \nu) \sum_{i=1}^n \left\| \hat{x}_i^t - \frac{1}{n} \sum_{j=1}^n \hat{x}_j^t \right\|^2. \end{aligned}$$

Telescoping the sum and using the tower rule of expectations, we get summability over t of the three negative terms above: for every $T \geq 0$, we have

$$(2 - \gamma \mathcal{L}) \sum_{i=1}^n \sum_{t=0}^T \mathbb{E}[D_{f_i}(x_i^t, x^*)] \leq \Psi^0 - \mathbb{E}[\Psi^{T+1}] \leq \Psi^0, \quad (39)$$

$$\gamma \sum_{i=1}^n \sum_{t=0}^T \mathbb{E}[\|h_i^t - h_i^*\|^2] \leq \Psi^0 - \mathbb{E}[\Psi^{T+1}] \leq \Psi^0, \quad (40)$$

$$\frac{\rho}{\gamma} (1 - \nu - \chi) \sum_{i=1}^n \sum_{t=0}^T \mathbb{E} \left[\left\| \hat{x}_i^t - \frac{1}{n} \sum_{j=1}^n \hat{x}_j^t \right\|^2 \right] \leq \Psi^0 - \mathbb{E}[\Psi^{T+1}] \leq \Psi^0. \quad (41)$$

Taking ergodic averages and using convexity of the squared norm and of the Bregman divergence, we can now get $\mathcal{O}(1/T)$ rates. We use a tilde to denote averages over the iterations so far. That is, for every $i = 1, \dots, n$ and $T \geq 0$, we define

$$\tilde{x}_i^T := \frac{1}{T+1} \sum_{t=0}^T x_i^t$$

and

$$\tilde{x}^T := \frac{1}{n} \sum_{i=1}^n \tilde{x}_i^T.$$

The Bregman divergence is convex in its first argument, so that, for every $T \geq 0$,

$$\sum_{i=1}^n D_{f_i}(\tilde{x}_i^T, x^*) \leq \sum_{i=1}^n \frac{1}{T+1} \sum_{t=0}^T D_{f_i}(x_i^t, x^*).$$

Combining this inequality with (39) yields, for every $T \geq 0$,

$$(2 - \gamma \mathcal{L}) \sum_{i=1}^n \mathbb{E}[D_{f_i}(\tilde{x}_i^T, x^*)] \leq \frac{\Psi^0}{T+1}. \quad (42)$$

Similarly, for every $i = 1, \dots, n$ and $T \geq 0$, we define

$$\tilde{h}_i^T := \frac{1}{T+1} \sum_{t=0}^T h_i^t$$

and we have, for every $T \geq 0$,

$$\sum_{i=1}^n \left\| \tilde{h}_i^T - h_i^* \right\|^2 \leq \sum_{i=1}^n \frac{1}{T+1} \sum_{t=0}^T \|h_i^t - h_i^*\|^2.$$

Combining this inequality with (40) yields, for every $T \geq 0$,

$$\gamma \sum_{i=1}^n \mathbb{E} \left[\left\| \tilde{h}_i^T - h_i^* \right\|^2 \right] \leq \frac{\Psi^0}{T+1}. \quad (43)$$

Finally, for every $i = 1, \dots, n$ and $T \geq 0$, we define

$$\tilde{x}_i^T := \frac{1}{T+1} \sum_{t=0}^T \hat{x}_i^t$$

and

$$\tilde{x}^T := \frac{1}{n} \sum_{i=1}^n \tilde{x}_i^T,$$

and we have, for every $T \geq 0$,

$$\sum_{i=1}^n \left\| \tilde{x}_i^T - \tilde{x}^T \right\|^2 \leq \sum_{i=1}^n \frac{1}{T+1} \sum_{t=0}^T \left\| \hat{x}_i^t - \frac{1}{n} \sum_{j=1}^n \hat{x}_j^t \right\|^2.$$

Combining this inequality with (41) yields, for every $T \geq 0$,

$$\frac{p}{\gamma} (1 - \nu - \chi) \sum_{i=1}^n \mathbb{E} \left[\left\| \tilde{x}_i^T - \tilde{x}^T \right\|^2 \right] \leq \frac{\Psi^0}{T+1}. \quad (44)$$

Next, we have, for every $i = 1, \dots, n$ and $T \geq 0$,

$$\begin{aligned} \left\| \nabla f(\tilde{x}_i^T) \right\|^2 &\leq 2 \left\| \nabla f(\tilde{x}_i^T) - \nabla f(\tilde{x}^T) \right\|^2 + 2 \left\| \nabla f(\tilde{x}^T) \right\|^2 \\ &\leq 2\mathcal{L}^2 \left\| \tilde{x}_i^T - \tilde{x}^T \right\|^2 + 2 \left\| \nabla f(\tilde{x}^T) \right\|^2. \end{aligned} \quad (45)$$

Moreover, for every $T \geq 0$ and solution x^* to (1),

$$\begin{aligned} \left\| \nabla f(\tilde{x}^T) \right\|^2 &= \left\| \nabla f(\tilde{x}^T) - \nabla f(x^*) \right\|^2 \\ &\leq \frac{1}{n} \sum_{i=1}^n \left\| \nabla f_i(\tilde{x}^T) - \nabla f_i(x^*) \right\|^2 \\ &\leq \frac{2}{n} \sum_{i=1}^n \left\| \nabla f_i(\tilde{x}^T) - \nabla f_i(\tilde{x}_i^T) \right\|^2 + \frac{2}{n} \sum_{i=1}^n \left\| \nabla f_i(\tilde{x}_i^T) - \nabla f_i(x^*) \right\|^2 \\ &\leq \frac{2\mathcal{L}^2}{n} \sum_{i=1}^n \left\| \tilde{x}_i^T - \tilde{x}^T \right\|^2 + \frac{4\mathcal{L}}{n} \sum_{i=1}^n D_{f_i}(\tilde{x}_i^T, x^*). \end{aligned} \quad (46)$$

There remains to control the terms $\|\tilde{x}_i^T - \tilde{x}^T\|^2$: we have, for every $T \geq 0$,

$$\begin{aligned} \sum_{i=1}^n \|\tilde{x}_i^T - \tilde{x}^T\|^2 &\leq 2 \sum_{i=1}^n \left\| (\tilde{x}_i^T - \tilde{x}^T) - (\tilde{x}_i^T - \tilde{x}^T) \right\|^2 + 2 \sum_{i=1}^n \left\| \tilde{x}_i^T - \tilde{x}^T \right\|^2 \\ &\leq 2 \sum_{i=1}^n \left\| \tilde{x}_i^T - \tilde{x}_i^T \right\|^2 + 2 \sum_{i=1}^n \left\| \tilde{x}_i^T - \tilde{x}^T \right\|^2. \end{aligned} \quad (47)$$

For every $i = 1, \dots, n$ and $t \geq 0$,

$$\hat{x}_i^t = x_i^t - \gamma(\nabla f_i(x_i^t) - h_i^t)$$

so that, for every $i = 1, \dots, n$ and $T \geq 0$,

$$\tilde{x}_i^T - \tilde{x}_i^T = \gamma \frac{1}{T+1} \sum_{t=0}^T \nabla f_i(x_i^t) - \gamma \tilde{h}_i^T$$

and

$$\begin{aligned} \left\| \tilde{x}_i^T - \tilde{x}_i^T \right\|^2 &= \gamma^2 \left\| \frac{1}{T+1} \sum_{t=0}^T \nabla f_i(x_i^t) - \tilde{h}_i^T \right\|^2 \\ &\leq 2\gamma^2 \frac{1}{T+1} \sum_{t=0}^T \left\| \nabla f_i(x_i^t) - \nabla f_i(x^*) \right\|^2 + 2\gamma^2 \left\| \tilde{h}_i^T - h_i^* \right\|^2 \\ &\leq 4\mathcal{L}\gamma^2 \frac{1}{T+1} \sum_{t=0}^T D_{f_i}(x_i^t, x^*) + 2\gamma^2 \left\| \tilde{h}_i^T - h_i^* \right\|^2. \end{aligned} \quad (48)$$

Combining (45), (46), (47), (48), we get, for every $T \geq 0$,

$$\begin{aligned} \sum_{i=1}^n \left\| \nabla f(\tilde{x}_i^T) \right\|^2 &\leq 2\mathcal{L}^2 \sum_{i=1}^n \left\| \tilde{x}_i^T - \tilde{x}^T \right\|^2 + 2n \left\| \nabla f(\tilde{x}^T) \right\|^2 \\ &\leq 2\mathcal{L}^2 \sum_{i=1}^n \left\| \tilde{x}_i^T - \tilde{x}^T \right\|^2 + 2\mathcal{L}^2 \sum_{i=1}^n \left\| \tilde{x}_i^T - \tilde{x}^T \right\|^2 + 4\mathcal{L} \sum_{i=1}^n D_{f_i}(\tilde{x}_i^T, x^*) \\ &= 4\mathcal{L}^2 \sum_{i=1}^n \left\| \tilde{x}_i^T - \tilde{x}^T \right\|^2 + 4\mathcal{L} \sum_{i=1}^n D_{f_i}(\tilde{x}_i^T, x^*) \\ &\leq 8\mathcal{L}^2 \sum_{i=1}^n \left\| \tilde{x}_i^T - \tilde{x}_i^T \right\|^2 + 8\mathcal{L}^2 \sum_{i=1}^n \left\| \tilde{x}_i^T - \tilde{x}^T \right\|^2 + 4\mathcal{L} \sum_{i=1}^n D_{f_i}(\tilde{x}_i^T, x^*) \\ &\leq 32\mathcal{L}^3\gamma^2 \frac{1}{T+1} \sum_{i=1}^n \sum_{t=0}^T D_{f_i}(x_i^t, x^*) + 16\mathcal{L}^2\gamma^2 \sum_{i=1}^n \left\| \tilde{h}_i^T - h_i^* \right\|^2 \\ &\quad + 8\mathcal{L}^2 \sum_{i=1}^n \left\| \tilde{x}_i^T - \tilde{x}^T \right\|^2 + 4\mathcal{L} \sum_{i=1}^n D_{f_i}(\tilde{x}_i^T, x^*). \end{aligned}$$

Taking the expectation and using (39), (43), (44) and (42), we get, for every $T \geq 0$,

$$\begin{aligned}
\sum_{i=1}^n \mathbb{E} \left[\|\nabla f(\tilde{x}_i^T)\|^2 \right] &\leq 32\mathcal{L}^3\gamma^2 \frac{1}{T+1} \sum_{i=1}^n \sum_{t=0}^T \mathbb{E} [D_{f_i}(x_i^t, x^*)] \\
&\quad + 16\mathcal{L}^2\gamma^2 \sum_{i=1}^n \mathbb{E} \left[\|\tilde{h}_i^T - h_i^*\|^2 \right] \\
&\quad + 8\mathcal{L}^2 \sum_{i=1}^n \mathbb{E} \left[\|\tilde{x}_i^T - \tilde{x}^T\|^2 \right] + 4\mathcal{L} \sum_{i=1}^n \mathbb{E} [D_{f_i}(\tilde{x}_i^T, x^*)]. \\
&\leq \frac{32\mathcal{L}^3\gamma^2}{2-\gamma\mathcal{L}} \frac{\Psi_0}{T+1} + 16\mathcal{L}^2\gamma \frac{\Psi_0}{T+1} + \frac{8\mathcal{L}^2\gamma}{p(1-\nu-\chi)} \frac{\Psi_0}{T+1} + \frac{4\mathcal{L}}{2-\gamma\mathcal{L}} \frac{\Psi_0}{T+1} \\
&= \left[\frac{32\mathcal{L}^3\gamma^2 + 4\mathcal{L}}{2-\gamma\mathcal{L}} + 16\mathcal{L}^2\gamma + \frac{8\mathcal{L}^2\gamma}{p(1-\nu-\chi)} \right] \frac{\Psi_0}{T+1}.
\end{aligned}$$

□

Hence, with $\gamma = \Theta\left(\frac{p}{\mathcal{L}}\sqrt{\frac{c}{n}}\right)$, χ satisfying $\delta \leq \chi \leq 1 - \nu - \delta$ for some $\delta > 0$, and $h_i^0 = \nabla f_i(x^0)$, for every $i \in [n]$, then for every $\epsilon > 0$, we have

$$\sum_{i=1}^n \mathbb{E} \left[\|\nabla f(\tilde{x}_i^T)\|^2 \right] \leq \epsilon \tag{49}$$

after

$$\mathcal{O} \left(\frac{\mathcal{L}^2}{p} \sqrt{\frac{n}{c}} \frac{\|\mathbf{x}^0 - \mathbf{x}^*\|^2}{\epsilon} \right) \tag{50}$$

iterations and

$$\mathcal{O} \left(\mathcal{L}^2 \sqrt{\frac{n}{c}} \frac{\|\mathbf{x}^0 - \mathbf{x}^*\|^2}{\epsilon} \right) \tag{51}$$

communication rounds.

We note that LT does not yield any acceleration: the communication complexity is the same whatever p . CC is effective, however, since we communicate much less than d floats during every communication round.

This convergence result applies to Algorithm 2. \tilde{x}_i^T in (36) is an average of all x_i^t , including the ones for clients not participating in the next communication round. The result still applies to **TAMUNA**, with, for every $i \in [n]$, \tilde{x}_i^T defined as the average of the $x_i^{(r,\ell)}$ which are actually computed, since this is a random subsequence of all x_i^t .